Leisure Boat Concept Design: Study on the Influence of Hull Form and Dimension to Increase Hydrodynamic Performance

Mukhammad Afit Lutfi [1], Aditya Rio Prabowo [1,*], Emel Mixsa Muslimy [2], Teguh Muttaqie [3], Nurul Muhayat [1], Hananta Diatmaja [1], Quang Thang Do [4], Seung Jun Baek [5], and Aldias Bahatmaka [6]

[1] Department of Mechanical Engineering, Universitas Sebelas Maret, Surakarta 57126, Indonesia
[2] Marathon Pacific Marines Co. Ltd., Tangerang 15510, Indonesia
[3] Research Center for Hydrodynamics Technology, National Research and Innovation Agency (BRIN), Surabaya 60112, Indonesia
[4] Department of Naval Architecture and Ocean Engineering, Nha Trang University, Nha Trang, 650000, Viet Nam
[5] Advanced-Green Technology Center, Korea Marine Equipment Research Institute, Busan 46744, South Korea
[6] Department of Mechanical Engineering, Universitas Negeri Semarang, 50229 Semarang, Indonesia
Email: afittj@student.uns.ac.id (M.A.L.); aditya@ft.uns.ac.id (A.R.P.); emixsa19@gmail.com (E.M.M.); teguh.muttaqie@brin.go.id (T.M.); nurulmuhayat@staff.uns.ac.id (N.M.); hananta037@student.uns.ac.id (H.D.); thangdq@ntu.edu.vn (Q.T.D.); sjbaek@komeri.re.kr (S.J.B.); aldiasbahatmaka@mail.unnes.ac.id (A.B.)
*Corresponding author

***Abstract*—The tourism sector contributes significantly to the economic growth of the community and the country. Labuan Bajo has the potential for marine tourism, which is famous for foreign classes. The separation of the islands in Labuan Bajo requires transportation to support tourist activities to tourist destinations. One type of transportation to support the needs of marine tourism is leisure boats or recreational boats. The leisure ship must have standards of comfort, security for passenger safety, and efficient operational costs. It is necessary to have infrastructure in the form of a leisure ship that functions optimally, so research on the hull's hydrodynamic characteristics is essential. This research aims to observe the influence of hull form variables and primary size on the hydrodynamic characteristics of the ship. The research method was the simulation method to determine the response of the hull model variation to the environmental conditions tested. Simulation testing using Maxsurf software based on resistance, stability, and seakeeping criteria. The MADM method analysis results showed that the Deep V Hull model variation had the highest score of 0.787. In the sensitivity analysis calculation, the hull form variable significantly affected resistance and stability testing with R square values of 0.6008 and 0.5930. Meanwhile, the size variable had more influence on seakeeping testing, especially roll motion, with an R square value of 0.4081.**

***Keywords*—Nautic tourism, leisure boat, hull form, main dimension, hydrodynamic criteria**

I. Introduction

Tourism is a strategic sector that contributes to economic growth, encourages, and creates jobs, develops investment, and increases people's income [1]. The Indonesian government plans for tourism to contribute to GDP growth and employment, with a target of 12% of GDP by 2027 [2]. As one of the tourist destinations in Indonesia, Labuan Bajo is targeted by the central government to become a Special Economic Zone (SEZ), which is expected to impact economic growth in the area [3]. Separating small islands in the Labuan Bajo region makes transportation modes important for connecting tourists to scattered tourist destinations [4].

Ships used in tourism activities must have safety standards for passenger safety and be cost-efficient for their owners [5]. The number of recorded tourist vessel accidents is still relatively high, with more than 4,000 cases reported in 2014 and many more accidents not reported (USCG, 2014) [6]. A study in the Turkish Aegean Sea mentioned that the type of ship with the most accidents was yachts/leisure boats, with the most common type of failure being hull/engine failure [7]. Therefore, an optimally functioning leisure ship is needed to facilitate marine tourism activities, especially in the Labuan Bajo Special Economic Zone (SEZ), Indonesia.

As a means of transportation, ships have a charm not owned by other modes of transportation. To increase the value of tourist engagement in tourist areas, build adequate infrastructure [8]. The publication of The Travel and Tourism Competitiveness Report by the World Economic Forum (WEF) in 2019 revealed that Indonesia's tourism competitiveness index globally ranked 40 out of 140 countries. However, Indonesia's competitiveness ranking in the infrastructure sector is only 71 [9]. There needs to be more in the global ranking index and tourism infrastructure. To catch up, improvements are needed in the tourism infrastructure

Manuscript received August 29, 2023; revised September 25, 2023; accepted October 25, 2023; published February 21, 2024.

sector. One way that can be done is by developing a ship hull model.

In previous studies, researchers conducted studies on hull optimization to find hull shapes with good hydrodynamic performance [10–12]. Then, there is a study on the effect of hull appendage on ship resistance value [13]. Research on monohull hull types with different dimensions produced diverse hydrodynamic characteristic data [14]. Research on ship hydrodynamic performance, including resistance, stability, and seakeeping, was conducted on regression analysis, scale, and reference design methods [15]. In the early phase of the design process, selecting hull type is an issue that must be carefully considered. The more advanced the science of naval architecture, the various types of hulls are developed according to their functions to obtain maximum performance.

This research focuses on the selection of hull types that compare resistance, stability, and seakeeping results with the regression analysis design method. Monohull hull types such as Flat Bottom, Deep V Hull, Shallow V, and Round Hull are the hull types to be evaluated. To produce a hull with the best performance, a more detailed hydrodynamic analysis is needed according to the needs of leisure boats. Comparison between hull designs using the Multi-attribute Decision Making (MADM) method. Furthermore, the sensitivity analysis method was carried out to determine the effect between variations in hull shape or size used.

II. Literature Review

A. Regression Method

The regression method is a method that can be used for two theories. First, regression methods are commonly used to estimate or predict data. Second, regression methods can be used in cases to determine the causal relationship between dependent and independent variables. In this method, the independent variable "*X*" is used to predict the outcome of the dependent variable "*Y*" [16]. Much research has been done using regression methods to predict key dimensions and particulars in shipping. Regression methods are used mainly in the early design phase to maximize certain ship design variables based on collected data [17]. Linear regression is one method to determine the relationship between the main dimensions of a ship by following a straight-line curve. The equation for the mathematical formula of simple linear regression is shown in Eq. (1) [16].

$$Y = aX + b \tag{1}$$

where *Y* and *X* are variables, a and b are constants.

B. Resistance Analysis

Regarding ship hydrodynamics, predicting total and component resistance on the ship when it is above the water surface is very important. Thus, the ship's adequate power and the main engine's power requirements can be estimated [18]. A boat moving on the water will have a force opposite to the direction of motion of the ship [19]. The ship resistance formula was developed by eliminating the incident wave area and only considering the available constant water flow that describes the combined wave and water flow forces [20]. Ship resistance includes frictional resistance, viscous pressure resistance, and wave resistance [21]. For low-speed ships, frictional resistance accounts for the most significant proportion of the total resistance [22, 23].

Frictional resistance is the total of the tangential frictional forces of the fluid acting on all elements of the hull surface exposed to water from the fore to aft [19]. The frictional resistance component is calculated based on the Reynolds number, wet surface area, and hull roughness allowance. The frictional resistance formula based on the International Towing Tank Conferences (ITTC) is presented in Eqs. (2) and (3) [24].

$$C_f = \frac{0.075}{(logR_n - 2)^2} \tag{2}$$

$$C_f = \frac{R_f}{\frac{1}{2}\rho S v^2} \tag{3}$$

where C_f is the coefficient of friction resistance, R_n is the Reynold number value, R_f is the friction resistance of the ship (N), ρ is the density of water (kg/m³), S is the wetted area (m²), and v is the ship speed (m/s).

Viscous resistance is the resistance that occurs due to the effect of fluid viscosity. The value of viscous resistance depends on the pressure distribution around the hull, which is influenced by wave resistance. Viscous resistance and viscous coefficient can be shown in Eqs. (4) and (5) [19].

$$R_v = \iint_{wake} \left\{ \Delta p + \frac{1}{2}\rho(u'^2 - u^2) \right\} dzdy \tag{4}$$

$$C_v = (1 + k)C_f \tag{5}$$

where R_V is the viscous resistance, C_V is the viscous resistance coefficient, k is the kinetic energy of turbulence (m²/s²), and C_f is the frictional resistance coefficient.

Wave resistance is caused by the energy transferred from the hull to the wave system [25]. At high speeds, wave resistance (R_W) has a small value. The wave resistance value is shown in Eq. (6) [26].

$$R_w = c_1 c_2 c_3 \nabla \rho g exp\{m_1 F_n^g + m_4 cos(\lambda F_r^{-2})\} \tag{6}$$

where R_W is the wave resistance (N), ∇ is the volume displaced of the ship (m³), g is the acceleration of gravity (m/s²), F_n is the Froude number value, and λ is the leeway angle (•).

C. Savitsky Method

The Savitsky method is widely used to evaluate drag for vessels with a planning hull type. It is based on the prismatic empirical equation and assumes that the part of

the hull in contact with water plans a constant cross-section. By determining the balance angle through iteration, this method takes into account the hull properties when predicting drag [27]. According to Savitsky, the total hydrodynamic drag of a planning hull can be formulated in the following Eq. (7) [28].

$$D = \Delta\, tan(\tau) + \frac{\varphi v^2 C_f \Delta B^2}{2\, cos(\beta) cos\,(\tau)} \quad (7)$$

where Δ is displacement, τ is trim angle, v is ship speed, B (beam) hull width, and β deadrise angle.

D. Froude Number

In the resistance test, the Froude number is a dimensionless number found in the flow around the hull [29]. The Froude number represents the ratio of inertial and gravitational forces associated with wave-making resistance. Froude number and hull shape significantly affect the convergence of the wave profile. The Froude number formula is shown in Eq. (8) [30].

$$F_n = \frac{v}{\sqrt{gL}} \quad (8)$$

where F_n is the Froude number, v is the ship's speed (m/s), L is the length of the ship's waterline (m), and g is the value of gravitational acceleration (9.81 m/s^2).

E. Reynolds Number

Reynold's number indicates the ratio of inertial force and viscous force. In addition, the Reynold number also shows the laminar, transient, or turbulent flow [31, 32]. When the Reynold number of the flow is less than the lower critical, the flow field is laminar. When the Reynold number of the flow is greater than the upper critical, the flow field is turbulent. When Reynold's number is between the lower and upper critical numbers, the flow is transient [33]. Reynold's number formula is expressed in Eq. (9) [34].

$$R_n = \frac{vL}{\mu} \quad (9)$$

where R_n is the value of Reynold's number, V is the ship's speed (m/s), L is the length of the ship's waterline (m), and v is the viscosity of water (m^2/s).

F. Stability Analysis

Ship stability is a part of naval architecture and ship design that deals with the behavior of ships at sea, both in calm and choppy conditions. Two types of ship stability approaches are intact stability and damage stability [35]. Intact stability is the ability to withstand external moments without affecting ship operations. Damage stability is the capability to maintain the ship from capsizing due to damage caused by external moments [36].

Righting Lever (GZ) curves are applied to determine the safety level of ships regulated in various regulations, including intact and damage stability. When a ship dives to an angle φ, the center of buoyancy shifts from point B0 to point $B\varphi$, and the center of gravity G may also shift in the presence of cargo. The buoyancy lift force Δ is equal to the weight of ship W, but the direction of this force is opposite. This pair of forces produces a righting moment. The righting lever GZ is the lateral distance between the center of gravity and the center of buoyancy force in the coordinates shown in the following Fig. 1 [37].

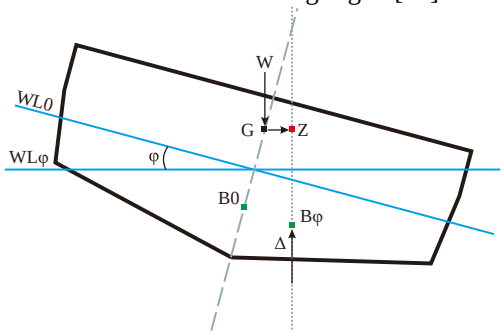

Fig. 1. Righting lever GZ at heel φ.

The main parameters on the righting lever curve for calculating stability criteria are stable heel angle, maximum righting lever, stability range, and area under righting lever GZ. The area under the GZ factor is the wet surface area under the righting lever curve calculated from the perpendicular position to a specific slope at the heel angle [38]. This factor is one of the references to ship stability. The stability reference criteria based on International Maritime Organization (IMO) A.749 (18) are as follows [39]:

- The area under the GZ curve up to an angle of 30° is not less than 0.055 m·rad or 3.151 m·deg.
- The area under the GZ curve up to an angle of 40° is not less than 0.09 m·rad or 5.517 m·deg
- The area under the GZ curve between an angle of 30° and 40° is not less than 0.03 m·rad or 1.719 m·deg.
- The GZ arm at heel angles equal to or greater than 30° shall not be less than 0.2 m.
- The maximum GZ arm shall occur at a heel angle of not less than 25°
- Initial metacenter points height GM0 not less than 0.15 m.

Angle vanishing degree is the maximum tilt angle position when the GZ condition switches to negative. The points of gravity and buoyancy are vertically aligned due to unstable equilibrium conditions [36]. When the ship's tilt exceeds the angle vanishing degree, the ship's stability capability will not be able to restore the ship's upright position.

G. Seakeeping Analysis

Ship seakeeping directly affects all ships' habitability, usability, and safety. In the design phase, it is crucial to accurately predict the ship's seakeeping behavior under real ocean conditions [40]. The ship's motion response to regular and irregular waves can be determined from motion analysis, namely seakeeping analysis and maneuvering analysis. Seakeeping analysis consists of

three motions: heaving, rolling, and pitching. While the maneuvering analysis considers three other degrees of freedom, namely surging, swaying, and yawing, as shown in Fig. 2 [41]. Of the six types of motions, only three are affected by acceleration and have a return force, namely heaving, rolling, and pitching [42].

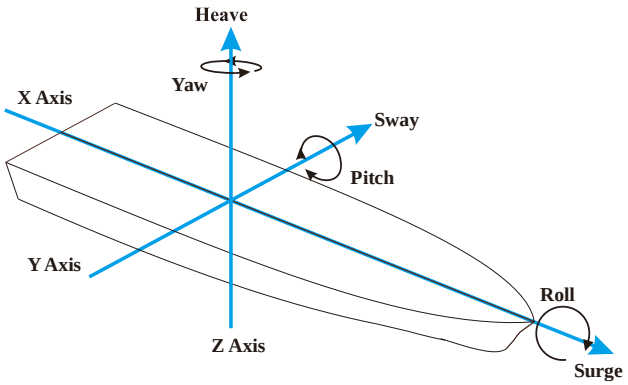

Fig. 2. Six degrees motion of ship.

Heave motion is the up and down of the ship parallel to the z-axis due to waves. The following Eq. (10) is used to determine the heave motion [43].

$$a\ddot{z} + b\dot{z} + cz = F_0 Cos\omega_\theta t \quad (10)$$

where $a\ddot{z}$ is inertial force, $b\dot{z}$ is damping force, cz is restoring force, and F_0Cos $\omega_\theta t$ is exciting force.

Roll motion is the ship's movement around the x-axis due to waves coming from the ship's side. The roll motion is analyzed using Eq. (11) [43].

$$a\frac{d^2\emptyset}{dt^2} + a\frac{d\emptyset}{dt} + c\emptyset = M_o \cdot Cos\omega_\theta t \quad (11)$$

where $a\frac{d^2\emptyset}{dt^2}$ is inertial force, $a\frac{d\emptyset}{dt}$ is damping force, $c\emptyset$ is restoring force, and $M_o \cdot \cos\omega_\theta t$ is exciting force.

Pitch motion is the motion of the ship around the y-axis. This motion can happen due to waves that cause a difference in height between the fore and aft of the hull. The following Eq. (12) is used to determine the pitching motion [43].

$$d\ddot{\emptyset} + e\emptyset + h\emptyset = M_0 \cdot \mathrm{Cos}\omega_e t \quad (12)$$

where $d\ddot{\emptyset}$ is inertial force, $e\emptyset$ is damping force, $h\emptyset$ is restoring force, and $M_0 \cdot \mathrm{Cos}\omega_e t$ is exciting force.

H. Motion Sickness Incidence

The main parameter for predicting passenger comfort on board is the vertical acceleration of the ship combined with roll and pitch motions. Motion Sickness Incidence (MSI) is an index of the percentage of passengers who vomit after two hours of exposure to motion due to waves. The following Eq. (13) is used to calculate the MSI index [44]:

$$MSI = 100\left[0.5 + erf\left(\frac{log_{10}(0.798\sqrt{m_4}/g) - \mu_{MSI}}{0.4}\right)\right] \quad (13)$$

where m_4 is spectral moment of ship.

I. Response Amplitude Operator (RAO)

Response Amplitude Operators (RAO) is a transfer function-based system representing the relationship of a ship's response amplitude to the amplitude of ocean waves. RAO is generally determined in various wave directions and frequencies analytically, experimentally, or by the simulation to estimate the surge, sway, yaw, heave, roll, and pitch motion responses [45]. The following Eq. (14) is used to calculate the RAO value [15].

$$\mathrm{RAO} = \left(\frac{\emptyset_a}{\zeta_a}\right)^2 \quad (14)$$

where $\emptyset_a$ is the amplitude of ship motion response, and ζ_a is the amplitude of the incident wave (•).

J. Monohull Form Type

The hull shape significantly influences wave flow patterns and hydrodynamic characteristics of the ship [46]. In general, ship designs using monohull hull types have a variety of displacement hull (Round hull) and planning hull (Shallow V / Deep V / Flat Bottom hull) shapes according to the criteria for their intended use. Each hull form has its advantages and disadvantages.

The round hull type suits ship with much cargo and low speed. Round hull is one type of displacement hull, where most of the hull has good buoyancy [47]. This type of hull is semi-circular at the base. The round hull type will have higher stability when the center of gravity point is lower. To maintain the hull upright/stable, this ship requires an additional bilge keel on the side of the hull. An illustration of the round hull shape is shown in Fig. 3 below.

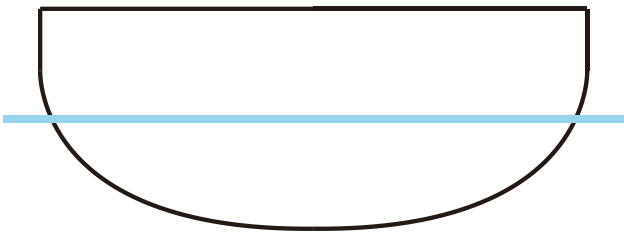

Fig. 3. Round hull.

The Deep V Hull has the most straightforward shape and excellent performance among the various hull types. Deep V Hulls can be applied to fast ferries, FACs, SWATHs, and catamarans. The main concept of the Deep V Hull is that there is a triangular midship section with a high deadrise angle (> 20°), a certain height of the chine in the bow area to avoid slamming and green water phenomena on the ship's deck, and the highest possible length-displacement ratio to reduce wave-resistance [48]. An illustration of the Deep V Hull shape is shown in Fig. 4 below.

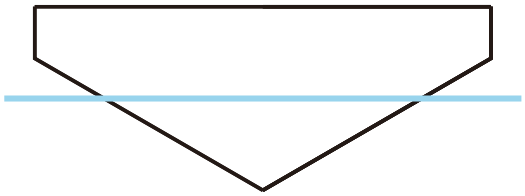

Fig. 4. Deep V Hull.

The shallow v hull type belongs to the planning hull category. Planning is a mode of operation for vessels whose weight is largely supported by hydrodynamic lift rather than buoyancy (hydrostatic lift). The dynamic lift reduces wetted surface area and resistance on the ship. The shallow v hull type is often used as a patrol boat, rescue boat, ambulance boat, offshore supply vessel, leisure/recreation boat, and for sports competitions. An illustration of the shallow V hull shape is shown in Fig. 5 below.

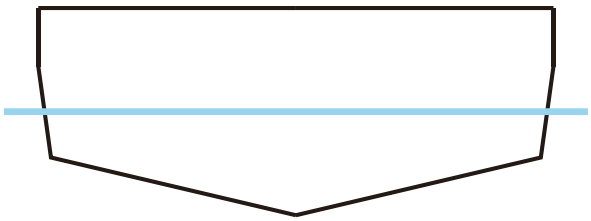

Fig. 5. Shallow V hull.

The flat bottom hull type is a design commonly used for small boats in shallow waters. Ships with this type of hull are often used by hunters or anglers in rivers or lagoons. This type of hull has disadvantages when used in deep or choppy waters because the flat base shape causes the ship to be prone to capsizing. An illustration of the flat bottom hull shape is shown in Fig. 6 below.

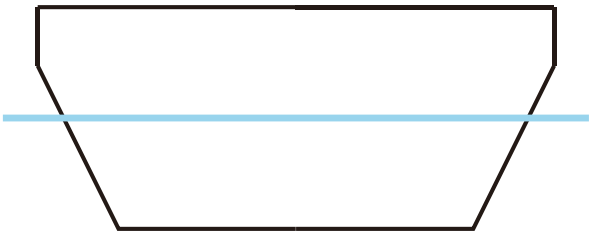

Fig. 6. Flat bottom hull.

K. *Multi Attribute Decision Making (MADM)*

Multi-Attribute Decision Making is a method of making conclusions or decisions from several available alternatives based on criteria with certain limitations [49]. This method uses simple weighting called Simple Additive Weighting (SAW), commonly used by practitioners [50]. The basic concept of the SAW method is to find the sum of the weights of the performance ratings for each alternative on all attributes. The SAW method requires normalization of the decision matrix (X) to a scale that can be compared with all existing alternative ratings. The normalization equation is shown in Eqs. (15) and (16) [15].

$$r_{ij} = \begin{cases} \frac{x_{ij}}{Max_i x_{ij}} \\ \frac{Min_i x_{ij}}{x_{ij}} \end{cases} \quad (15)$$

$$V_i = \sum_{j=1}^{n} w_i r_{ij} \quad (16)$$

where V is the preference value, w is criteria weight, and r is the normalized alternative value.

L. *Sensitivity Analysis*

Sensitivity analysis is an essential step in the modeling and results delivery process. Sensitivity analysis can help in seeing the changes in output against given inputs. An example is the model calibration process by optimizing the most influential experimental conditions to achieve accurate outcomes from the developed model [51]. Sensitivity tests are conducted to determine, obtain, and compare the results of the assessment criteria to determine the requirements that are most sensitive to changes in results [52–54].

III. Benchmarking

A. *Profile*

The validation carried out in this study is to replicate the research conducted by Rahmaji *et al.* [15]. The research conducted by Rahmaji *et al.* [15] is about improvising resistance, stability, and seakeeping capabilities in military patrol ship designs. The type of ship used was a fast patrol ship with a monohull hull type. Several design methods, such as regression, scaling, and reference methods, were applied in the study. Each method was compared with each other to determine the most effective method.

One of the ship sizes used by Rahmaji *et al.* [15] in their simulation was LOA 11.7 m, beam 4.2 m, depth 1.6 m, draft 0.7 m, and displacement 3.2 tons. The design used only displayed the hull's shape without being equipped with other supporting parts such as superstructure, inner construction, and propulsion. The research conducted by Rahmaji *et al.* already had complete information, making it easy to replicate. The ship design from the validation carried out can be seen in Fig. 7.

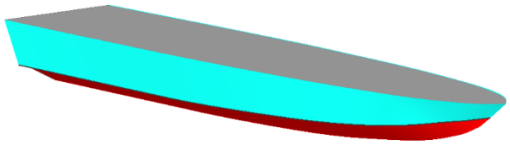

Fig. 7. Ship design validation.

Validation tests on the design include resistance, stability, and seakeeping simulations. The simulation running process uses Maxsurf Resistance, Maxsurf Stability, and Maxsurf Motion software. Each type of simulation has its boundary conditions.

B. *Validation Result*

Test validation can be accomplished by comparing the test results of each analysis. Fig. 8 shows the results of

simulation validation on resistance testing. For resistance simulation, the method used was Savitsky Planning, with a speed range of 0–50 knots.

Based on the Fig. 8, it can be seen that the amount of resistance on the hull is directly proportional to the additional speed of the ship. The higher the speed, the more excellent the resistance that the hull will receive. The simulation results that had been carried out were then compared with the test data from Rahmaji *et al.* [15] where the comparison graph of resistance and speed shows the same trend. Furthermore, hull stability testing was also carried out, simulated at the heel-to-starboard slope of 0° to 180°. Fig. 9 below shows the comparison of the stability analysis results.

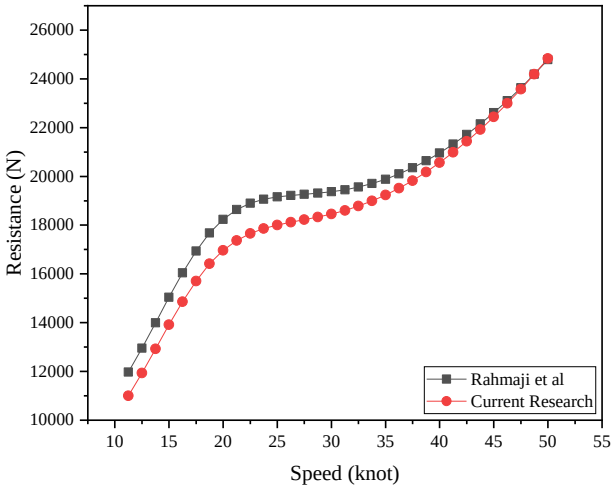

Fig. 8. Resistance testing validation.

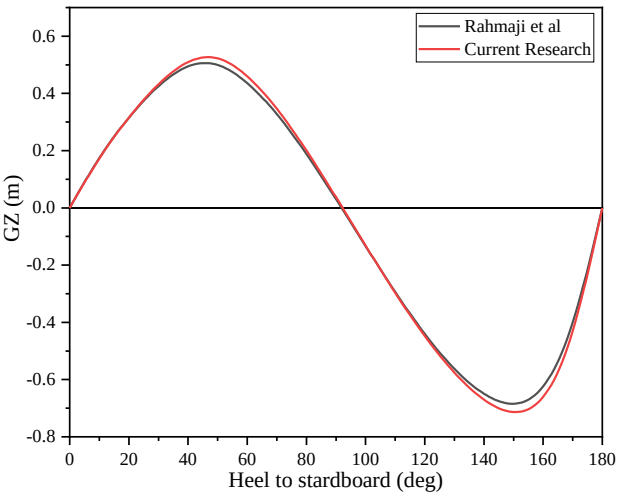

Fig. 9. Stability testing validation.

The comparison of the graphs above shows that the difference in stability curves between the research conducted by Rahmaji *et al.* [15] and the current research is similar. Simulations were conducted using the large angle stability method with a free trip to load case setup. The wave height condition entered followed the set height condition in the research reference, 1.875 m. The resulting curve trend was almost similar to the difference in the peak point area of the GZ curve. After testing the resistance and stability, the next step is to simulate the seakeeping of the hull. Fig. 10 shows the following RAO graphs in heave, roll, and pitch motion.

Seakeeping testing is conducted to provide insight into the response of the hull when passing through waves. Based on the results of the graph above, the difference in curves for each type of movement did not show a significant difference. The test results were in the condition of the incoming wave direction 135° (bow sea) with a ship speed of 10 knots. The roll motion curve had a difference in the wave frequency value but had the same line shape. Furthermore, the heave and pitch curves showed the same response characteristics, but there were differences in the amplitude of the movement. From all the tests carried out, the results of the validation data shown in Table I are as follows.

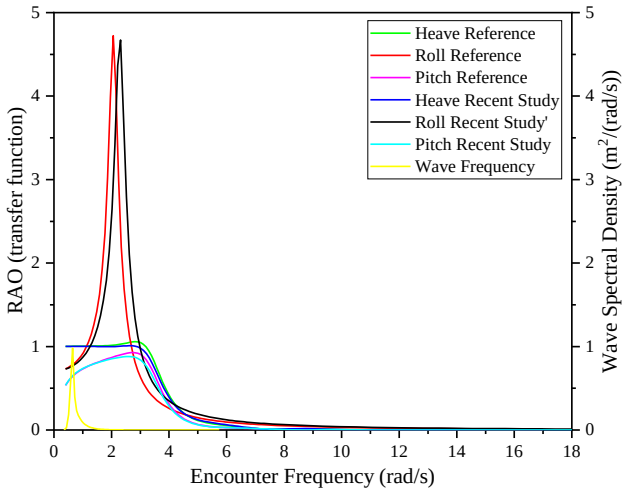

Fig. 10. Seakeeping testing validation.

TABLE I. VALIDATION RESULT

	Resistance	Stability	Seakeeping		
			Heave	Roll	Pitch
Rahmaji *et al.* [15]	19373.8	0.50	1.05	4.72	0.92
Current study	18619.34	0.52	1.00	4.67	0.88
Margin	4.05%	4.15%	4.68%	1.08%	4.5%

In the resistance test, the total resistance value produced by the current research was 18619.34 N, with a difference of 4.05% against the research reference. Then, in the stability simulation, the resulting max GZ was 0.50 m versus 0.52 m with a similar graphical shape. Furthermore, the seakeeping simulation that had been carried out showed a difference in results of 4.68%, 1.08%, and 4.5% for the types of heaves, roll, and pitch movements. The value was based on the amplitude of each movement. Based on the above data, all simulation results that had been carried out showed the same trend with a difference in results below 5% so that validation can be declared satisfactory and successful.

IV. METHODOLOGY

The research method consisted of several stages: data collection, data processing, simulation design, and data analysis. The reference vessels used were five leisure

vessels. Each stage in this research process is shown by the flowchart in Fig. 11. The reference ships were selected based on the actual ship size at the data collection stage. All reference ships entered the 3D modeling stage with Maxsurf Modeler software. Furthermore, the primary size data of the reference ship was processed with a regression approach.

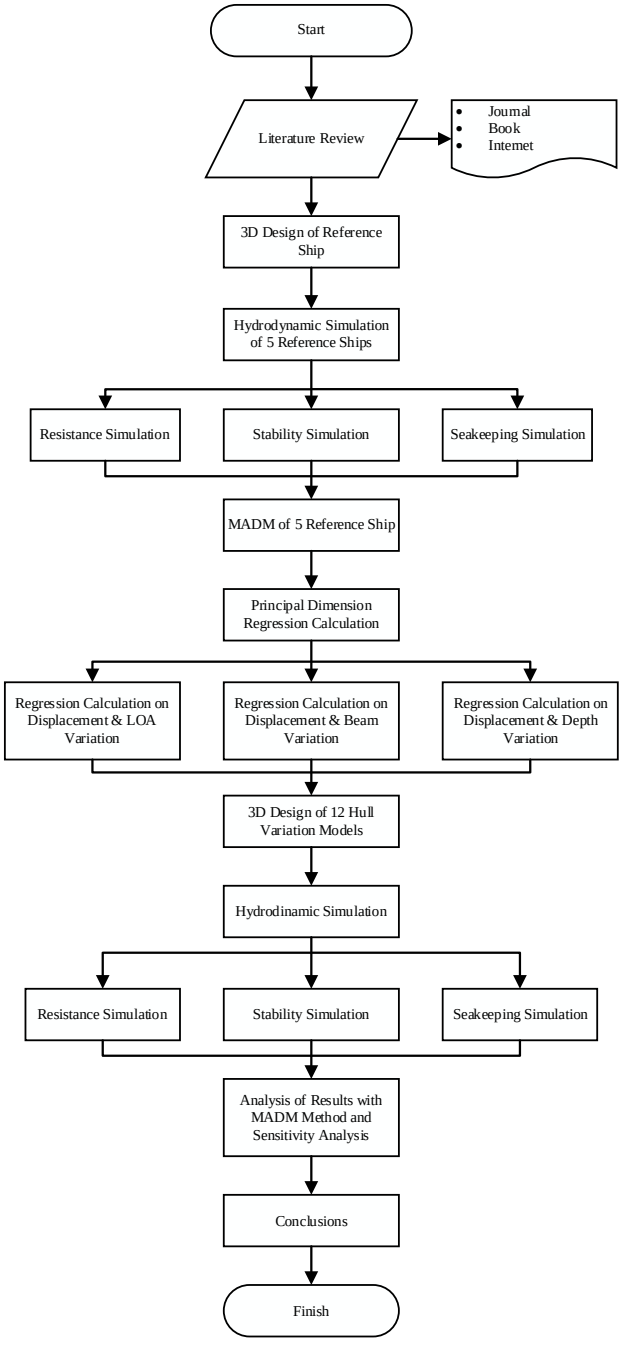

Fig. 11. Research flowchart.

The process results in one new main ship size from the regression results. After that, data processing was carried out again to find variations in the main size of the ship with a regression approach. The variation used was the regression result from locking three data: (a). displacement and LOA; (b). displacement and beam; c. displacement and depth. This stage will produce three variations of the main size of the ship. The next stage models four hull types (flat bottom, deep v, round hull, and shallow v).

Each hull type will be modeled on each primary dimension of the ship from the regression results of three data variations so that the combination of four hull types and three main sizes from regression will produce 12 ship models. The modeling process used Maxsurf Modeller software. All ship models will be simulated using Maxsurf Resistance, Maxsurf Stability, and Maxsurf Motion software.

This study ignored the effects of propulsion type and hull construction. From the analysis of 12 ship variations, the best alternative design model was evaluated using a simple weighting method of Multi-attribute Decision-Making (MADM). Then, a sensitivity analysis was conducted to find the effect of the input variables tested. The results of this study are expected to provide an evaluation of the leisure boat design method based on its hydrodynamic characteristics.

A. Ship Reference

The reference ship chosen is a type of leisure ship with a monohull type. Furthermore, looking for the principal dimension value with a range that is not far adrift from each other to produce a linear regression graph. The five reference ships that will be used are 27 Outlaw [55], 270 OSX [56], Leisure 28 [57], X26 [58], and DSCVR 9 [59]. The main dimensions of the reference ship are shown in Table II.

TABLE II. MAIN DIMENSION OF SHIP REFERENCES

Parameters	Ship reference				
	27 Outlaw	270 OSX	Leisure 28	X26	DSCVR 9
LOA (m)	8.47	8.23	8	8	8.57
Beam (m)	2.56	2.59	2.55	2.59	2.57
Depth (m)	1.4	1.6	1.4	1.6	1.78
Draft (m)	0.66	0.48	0.35	0.48	0.35
Disp.(ton)	2.37	2.04	1.65	3.13	2.25
LWL (m)	7.2	6.47	7.97	7.11	7.89
C_b (-)	0.34	0.33	0.3	0.39	0.39

In general, several parameters are used in the ship's main dimensions as the basis for ship architecture. These parameters are:

- Length Overall (LOA) is the overall length of the ship measured from bow to stern.
- Beam (B) is the width of the entire ship measured from the widest point.
- Depth (D) is the depth of the ship's hull measured from the deck to the keel
- Draft (T) is the height of the water level measured from the LWL line to the keel
- Displacement (Disp.) is the total weight of the ship with all its cargo
- Length Waterline (LWL) is the length of the ship's

waterline measured from the bow to the stern

- Coefficient block (Cb) is the ship's Carena volume ratio to the beam immersed in water.

After obtaining ship dimension data, the following process is to perform 3D modeling of the hull using Maxsurf Modeller software. Each reference hull is designed based on the specifications, size, shape, and line plan that have been made. The limitation in this hull modeling is only applying the hull's outer surface without including the construction structure factor. In addition, other supporting parts, such as the superstructure, interior layout, and ship propulsion system, are also not included in the hull modeling stage. So that the entire ship model only shows the hull's surface from the keel to the deck. The 3D design of the ship's hull is shown in Fig. 12.

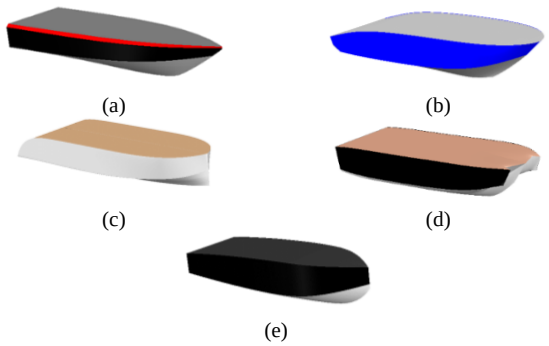

Fig. 12. Ship references: (a) 27 Outlaw; (b) 270 OSX; (c) Leisure 28; (d) X26; (e) DSCVR 9.

B. Ship References Analysis

Each reference vessel is simulated to find the best performance. The simulations carried out are resistance, stability, and seakeeping. The results of the analysis will be used in Multi-attribute Decision Making (MADM) calculations [60, 61]. The three reference ships with the top rank will be the reference in the following regression calculation method.

In resistance testing, each design is simulated as in an actual water environment. Some of the influencing factors include speed, hull shape, water draft, and ship size. All hull models were simulated under the same boundary conditions as in Table III. Resistance simulation is performed using Maxsurf Resistance software. The resistance testing results on the reference vessel are presented in Fig.13 and Tables IV and V.

Based on the resistance test results, the slightest resistance value at maximum speed is the 270 OSX, 27 Outlaw, Leisure 28, DSCVR 9, and X26. The total resistance values at the top speed are 7077.6 N, 8098.86 N, 8128.02 N, 8948.99 N, and 10445 N, respectively. Meanwhile, the required power is 325.51 hp, 372.48 hp, 373.82 hp, 411.58 hp, and 480.38 hp.

TABLE III. BASIC SETTING MAXSURF RESISTANCE

Resistance Boundary Condition	value
Method	Savitsky planning
Speed range	0–50 knot
efficiency	60%

TABLE IV. SPEED VS RESISTANCE

Model	Resistance (N)				
	V=10	V=20	V=30	V=40	V=50
27 Outlaw	3551.0	4274.0	4671.2	6029.7	8098.8
270 OSX	2840.7	3365.4	3860.9	5167.7	7077.6
Leisure 28	1151.3	2499.2	3835.2	5694.4	8128.0
X26	2501.8	4244.8	5454.4	7533.2	10445
DSCVR 9	1596.7	3089.2	4392.4	6335.8	8948.9

TABLE V. SPEED VS POWER

Model	Power (hp)				
	V=10	V=20	V=30	V=40	V=50
27 Outlaw	32.66	78.62	128.9	221.85	372.48
270 OSX	26.13	61.91	106.54	190.13	325.51
Leisure 28	10.59	45.97	105.83	209.52	373.82
X26	23.01	78.09	150.51	277.17	480.38
DSCVR 9	14.68	56.83	121.2	233.11	411.58

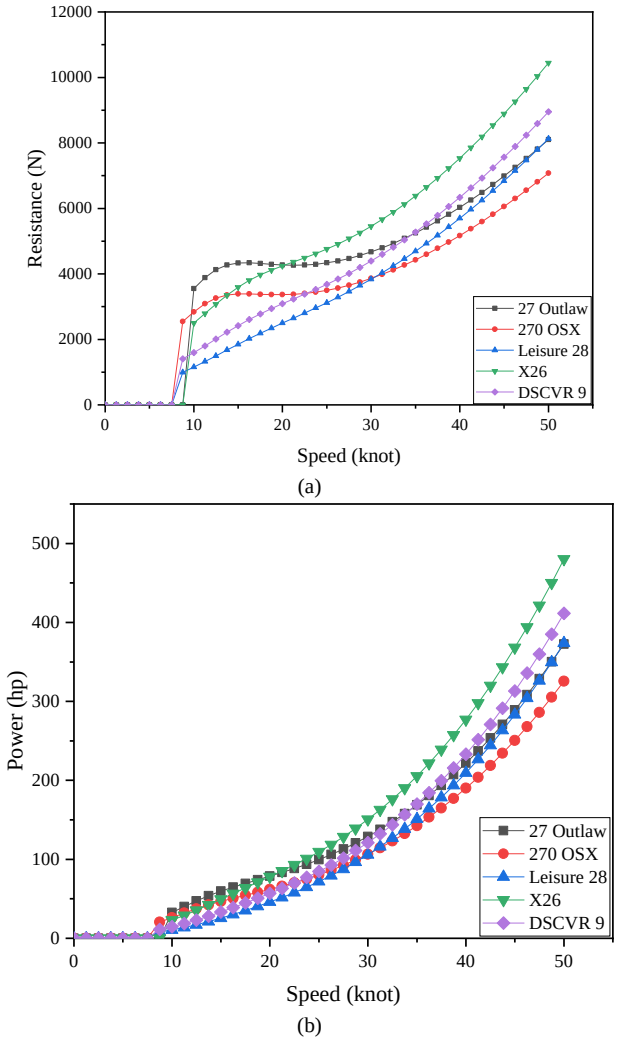

Fig. 13. Resistance graph of five reference ships: (a) Speed vs Resistance; and (b) Speed vs Power.

The next test performed is stability simulation. To determine the stability ability of the hull, the method used is static stability testing. The test process is carried out by rotating the ship on the x-axis at a specified tilt angle.

Under these conditions, several aspects of stability parameters that indicate the stability ability of the hull will be calculated. The hull stability capability test uses the help of Maxsurf Stability software. All hull models are simulated with the same boundary conditions as in Table VI. The stability test results will be presented in the GZ curve graph in Fig. 14 below.

Based on the stability testing results, the ship with the highest maximum GZ value is 270 OSX with a value of 0.366 m at an angle of 60°. In contrast, the lowest maximum GZ value is Leisure 28, with a value of 0.164 m at an angle of 20°.

TABLE VI. BASIC SETTING MAXSURF STABILITY

Stability Boundary Condition	value
Method	Large angle stability
Heel	0–180
Trim	Free trim to loadcase
Fluid	Simulate fluid movement
Density	Sea water (1025.0 kg/m^3)
Wave form	Sinusoidal (height 1.4 m)
Hog and Sag	Not applied
Water on deck	Not applied

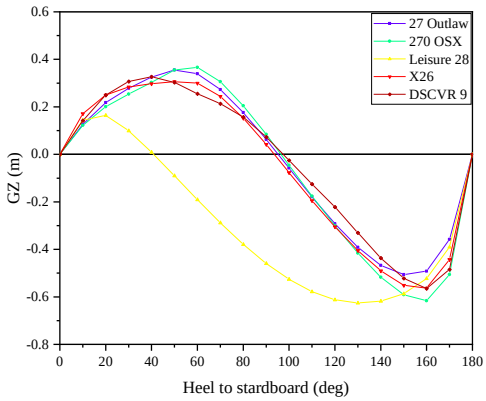

Fig. 14. GZ curve of five reference ships.

The next test is a seakeeping analysis of the ship model to determine the ship's motion. The ship has six motion degrees of freedom in its movement: heaving, rolling, pitching, surging, swaying, and yawing. In the seakeeping analysis, only three kinds of oscillatory movements are considered: heaving, rolling, and pitching. The limitation conditions tested in the seakeeping simulation are shown in Table VII. In the seakeeping analysis, RAO graphs of the three ship motions are in Fig. 15. For detailed configurations: the input for location is set according to COG position, 10 knot is defined as speed input, heading is assumed to be bow seas (135°), and spectra type is set as JONSWAP.

TABLE VII. BASIC SETTING MAXSURF MOTIONS

Seakeeping Boundary Condition	value
Analysis type	Strip theory
Vessel draft and trim	Zero trim
Vessel type	Monohull
Mass distribution	Automatic
Damping factors	Automatic
Environment	Sea water (1025.0 kg/m^3)
Frequency range	Automatic

In the heaving motion RAO graph, the ship with the highest motion response is X26. This ship has a maximum RAO value of 1.3 with an encounter frequency of 3.9 rad/s. Meanwhile, the ship with the lowest RAO is Leisure 28, with an RAO value of 1.04 and an encounter frequency of 3.9 rad/s. Then, in the rolling motion RAO graph, the ship with the highest motion response is 27 Outlaw with an RAO of 4.7 at an encounter frequency of 3.0 rad/s. The lowest rolling motion RAO value is DSCVR 9 of 4.5, with an encounter frequency of 3.0 rad/s. For the pitching motion RAO graph, the ship with the highest motion response is OSX 27. This ship has a maximum RAO value of 0.9 with an encounter frequency of 3.9 rad/s. Then for the lowest RAO value, Leisure 28 is 0.7 with an encounter frequency of 3.6 rad/s.

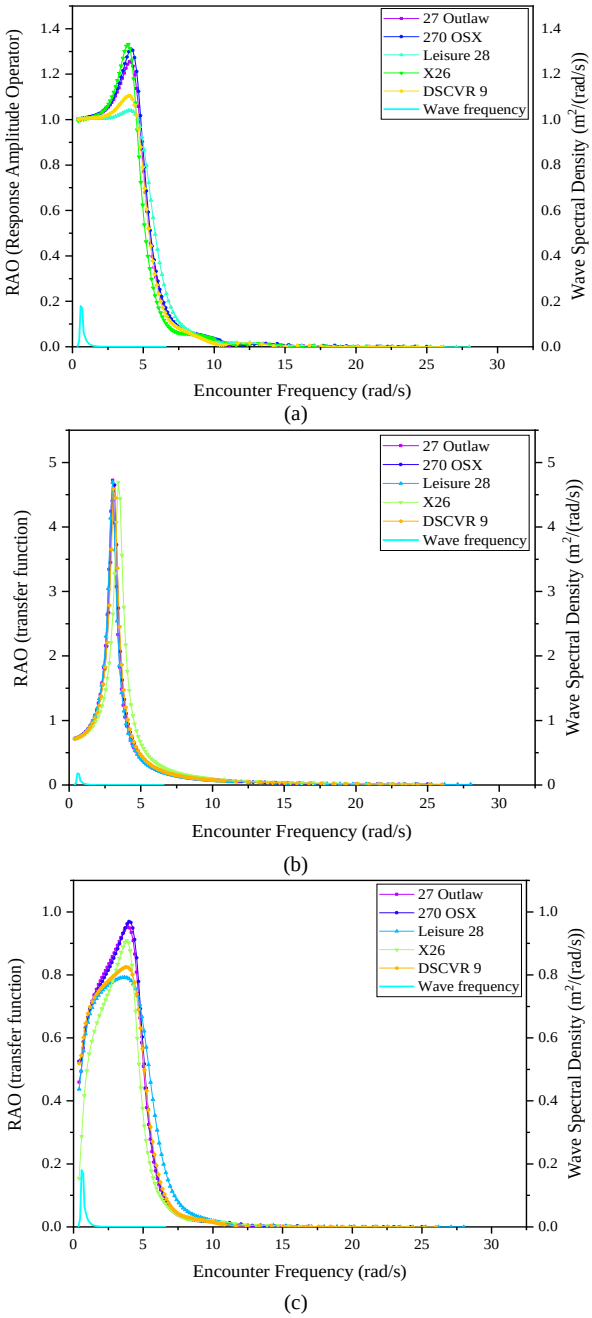

Fig. 15. Response Amplitude Operators (RAO): (a) heaving motion; (b) rolling motion; (c) pitching motion.

C. Multi Attribute Decision Making (MADM)

In the MADM calculation, the weights on the resistance, stability, and seakeeping parameter criteria are set according to the needs of the leisure boat. The weight of the criteria for each parameter is presented in Table VIII below.

TABLE VIII. WEIGHT CRITERIA

Criteria	Parameter	Weight
C1	Resistance	30%
C2	Stability	35%
C3	Seakeeping	35%

At the weighting stage, the resistance parameter gets smaller than the stability and seakeeping parameters. The stability factor gets a weight of 35% because the tour boat carries tourist passengers, so the safety factor is a priority. The seakeeping factor also gets a weight of 35% because the comfort factor of ship movement and the level of seasickness can be measured through the results of the seakeeping analysis. Then, the resistance factor gets a weight of 30% against the background of tourist ships that do not cover long distances and relatively low ship speeds. However, this factor is also crucial to consider in the calculation. The three criteria are used to determine the best reference ship based on simulation results. Simulation data from each parameter is taken to calculate the MADM method. Resistance data is taken at a ship speed of 10 knots, and stability is obtained from the angle of maximum GZ value. Meanwhile, seakeeping data comes from the average maximum heave, roll, and pitch motion values. Data for each parameter is presented in Table IX.

TABLE IX. PARAMETER VALUE FOR EACH CRITERIA

Ship Reference	Criteria		
	C1	C2	C3
27 Outlaw	2169.83	21.58	2.30
270 OSX	1757.84	22.02	2.30
Leisure 28	1683.17	4.33	2.17
X26	2435.26	20.57	2.30
DSCVR 9	1968.70	20.38	2.16

The next stage is normalization to avoid data anomalies. In criteria C1 and C3 (resistance and seakeeping), the smallest data is selected as a reference for normalization. For C2, the criteria are the opposite because a good ship design has a resistance value, a low seakeeping RAO peak point, and high stability. Normalization data for all reference ships are presented in Table X.

Based on the normalized data, the total value of each reference ship model is summed up. From the summation results, the best reference ship model can be determined based on MADM calculations. The results of the total value of all reference ship models are presented in Table XI.

TABLE X. DATA NORMALIZATION

Ship reference	Criteria		
	C1 (30%)	C2 (35%)	C3 (35%)
27 Outlaw	0.776	0.980	0.939
270 OSX	0.958	1.000	0.939
Leisure 28	1.000	0.197	0.996
X26	0.691	0.934	0.939
DSCVR 9	0.855	0.926	1.000

TABLE XI. MADM TOTAL VALUE

Ship Reference	Criteria			Total Value
	C1	C2	C3	
27 Outlaw	0.776	0.980	0.939	0.9045
270 OSX	0.958	1.000	0.939	0.9660
Leisure 28	1.000	0.197	0.996	0.7176
X26	0.691	0.934	0.939	0.8631
DSCVR 9	0.855	0.926	1.000	0.9304

From the sum of the total values, it can be concluded that the reference ship model with the best performance is 270 OSX with a final value of 0.96. The top three models from the ranking results of the MADM method calculation will be used to generate the main size in the regression method.

D. Regression Method

In ship design, the regression analysis method is applied to find the primary size data of the new design based on the collected reference ship data. The size is a variable relationship, namely displacement as the independent variable that produces the dependent variables LOA, beam, and depth [46]. The linear regression method used follows the mathematical model presented in Eq. (1). The correlation is displayed in the form of a straight-line curve that approximates the cause-and-effect variable. A graph of the regression results of the five reference ships is shown in Fig. 16.

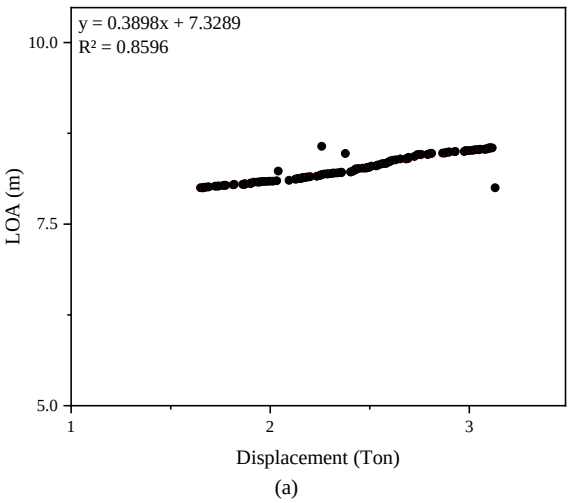

(a)

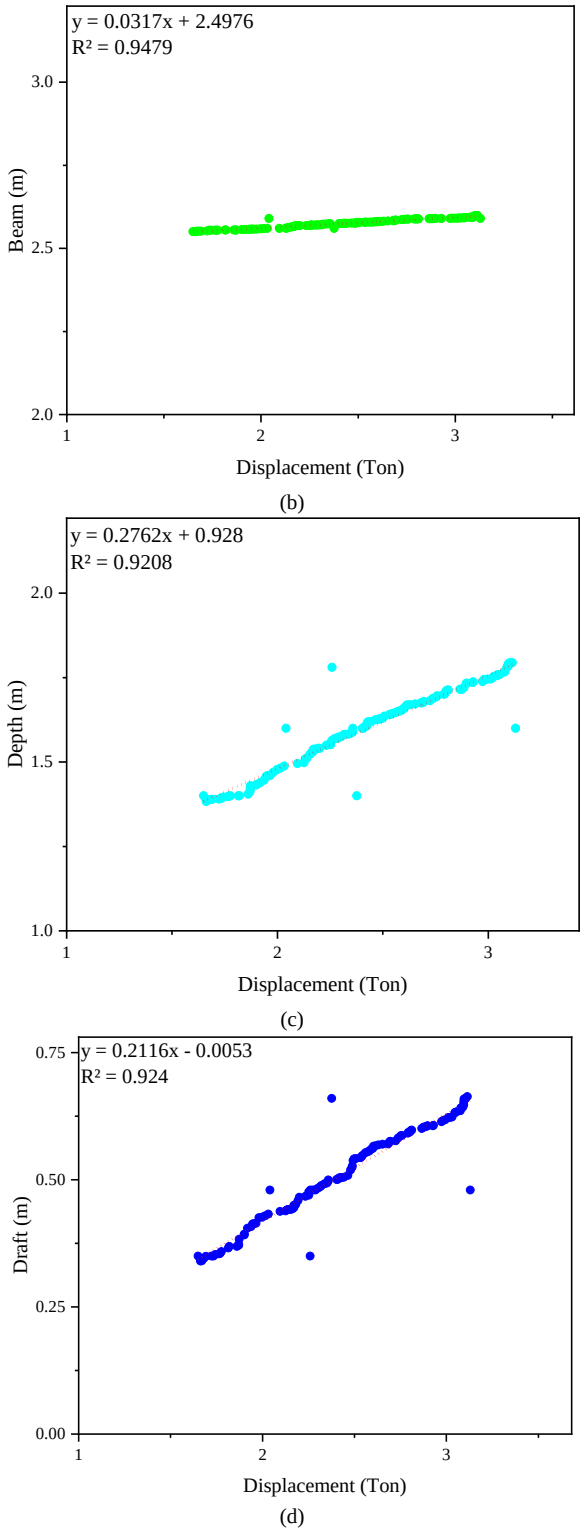

Fig. 16. Regression graph results: (a) LOA vs Displacement; (b) Beam vs Displacement; (c) Depth vs Displacement; and (d) Draft vs Displacement.

A straight-line equation was obtained from the linear regression results to identify the affected variables (LOA, beam, depth, and draft). The regression uses a target displacement of 2.29 tons derived from the average of the five reference ships. The next step is to find the value of the Y variable according to the straight-line equation in the graph in Fig. 16. The results of the calculation of the main dimensions of the new design are shown in Table XII.

TABLE XII. REGRESSION RESULT DIMENSION

Parameter	Value
LOA (m)	8.22
Beam (m)	2.57
Depth (m)	1.56
Draft (m)	0.48
Displacement (ton)	2.29

This study aims to analyze the effect of differences in main size on ship performance. The method used is to vary the results of the value of each regression calculation variable in Table XII into three new size variations. The three size variations are a. displacement and LOA, b. displacement and beam, c. displacement and depth. Each variable's value will be a fixed number, where the value of the other variables will be regressed again. The results of the regression method calculation on displacement and LOA variations are shown in Fig. 17, and the results of regression calculations on displacement and beam variations are shown in Fig. 18. Then, the results of regression calculations on displacement and depth variations are shown in Fig. 19.

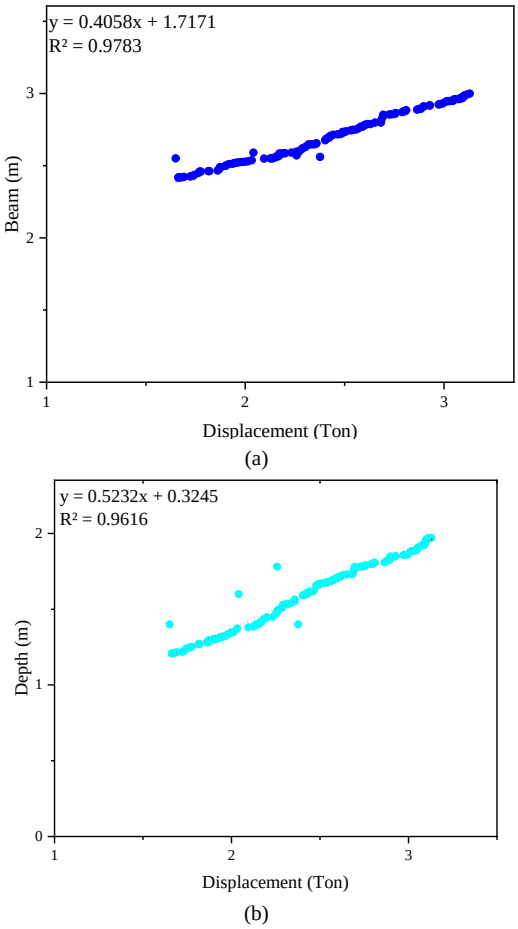

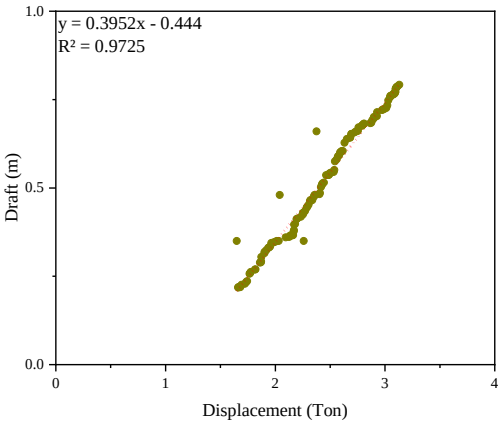

(c)

Fig. 17. Regression result graph with displacement and LOA variation: (a) beam vs displacement; (b) depth vs displacement; and (c) draft vs displacement.

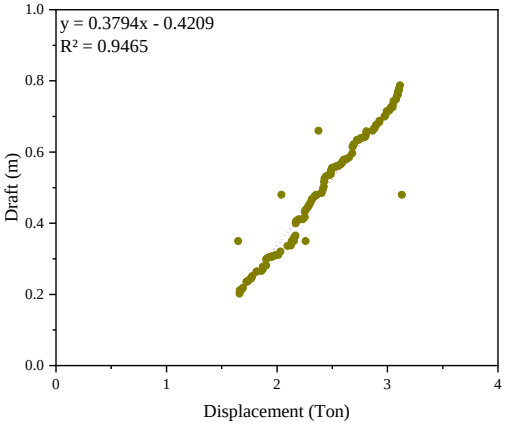

(c)

Fig. 18. Regression result graph with displacement and beam variation: (a) LOA vs displacement; (b) depth vs displacement; and (c) draft vs displacement.

Regression calculations for displacement and LOA variations produce three different values for the variables to be calculated: beam, depth, and draft. The LOA and displacement values for this dimension variation still use the same values as in Table XII. A recapitulation of the main dimension calculation results for this variation is presented in Table XIII.

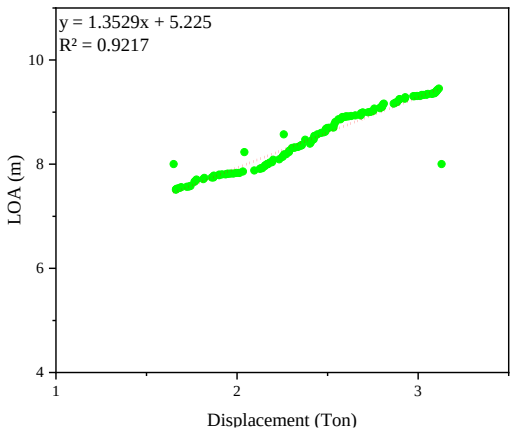

(a)

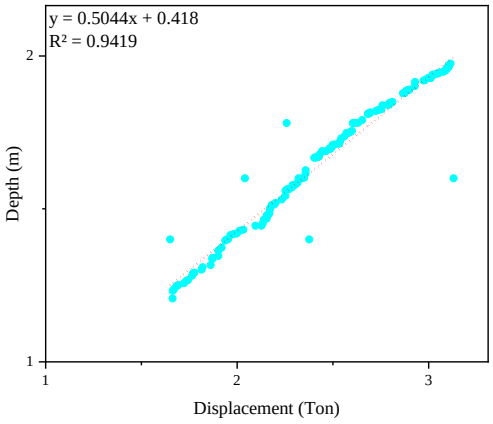

(b)

Regression calculations for displacement and beam variations produce three different values for calculating the variables: LOA, depth, and draft. We still use the same values as in Table XII for beam and displacement values in this size variation. A recapitulation of the main size calculation results for this variation is presented in Table XIII.

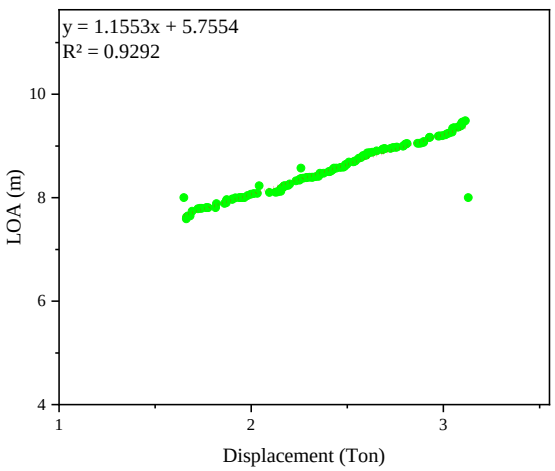

(a)

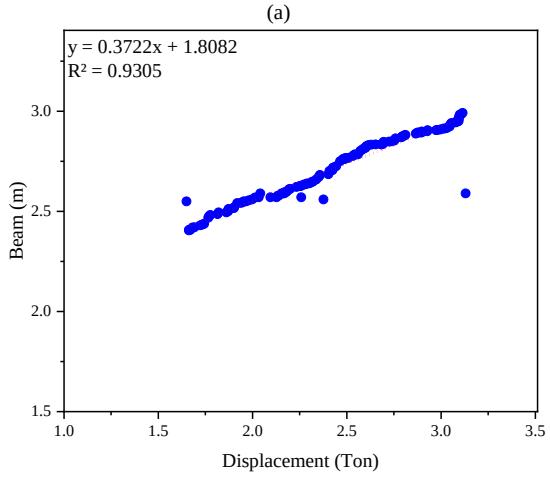

(b)

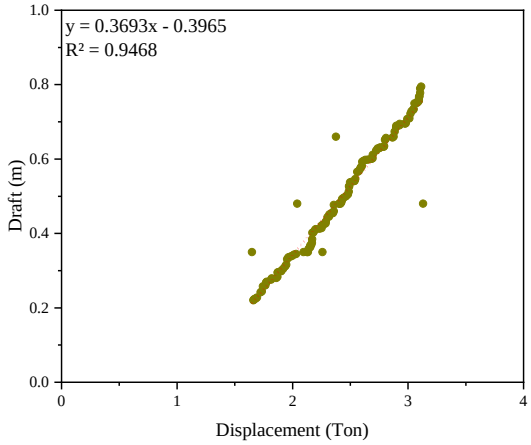

(c)

Fig. 19. Regression result graph with displacement and depth variation: (a) LOA vs displacement; (b) beam vs displacement; and (c) draft vs displacement.

Regression calculations for displacement and depth variations produce three different values for calculating the variables: LOA, beam, and draft. This dimension variation's depth and displacement values still use the same values as in Table XII. A recapitulation of the main dimension calculation results for this variation is presented in Table XIII.

TABLE XIII. RECAPITULATION OF THE MAIN DIMENSION PARAMETER VALUES OF THE REGRESSION OF VARIATION REGRESSION

Parameter	Parameter Variation according Regression		
	Disp. and LOA	Disp. and beam	Disp. and depth
LOA (m)	8.22	8.33	8.4
Beam (m)	2.65	2.57	2.66
Depth (m)	1.52	1.57	1.56
Draft (m)	0.46	0.45	0.45
Disp.(ton)	2.29	2.29	2.29

From the new dimensional data obtained, there are several changes from the initial regression dimensions in Table XII. The Displacement and LOA variation has a wider beam and a reduced depth value. Then, the Displacement and Beam variation have a longer LOA size and a higher depth value. In the Displacement and Depth variation, there is a change in the value of a longer LOA and a wider beam. Furthermore, 3D modeling variations are performed on four different hull types. The hull types to be used are flat bottom, deep v, round hull, and shallow v. The total number of ship models to be analyzed is 12. The 3D designs of each hull type and size variation are presented in Figs. 20–23.

(a) (b)

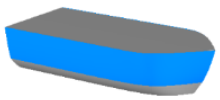

(c)

Fig. 20. Flat bottom hull design with dimensions: (a) Displacement and LOA; (b) Displacement and Beam; and (c) Displacement and Depth.

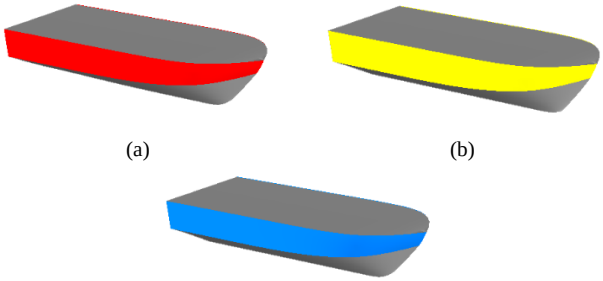

(a) (b)

(c)

Fig. 21. Deep V Hull design with dimensions: (a) Displacement and LOA; (b) Displacement and Beam; and (c) Displacement and Depth.

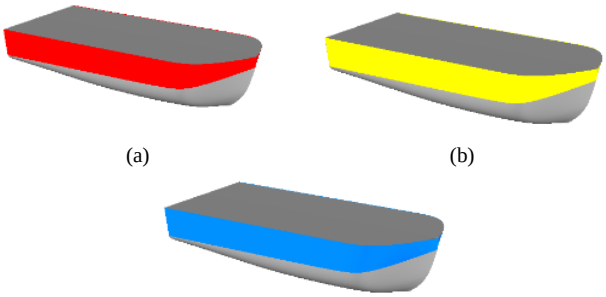

(a) (b)

(c)

Fig. 22. Round hull design with dimensions: (a) Displacement and LOA; (b) Displacement and Beam; and (c) Displacement and Depth.

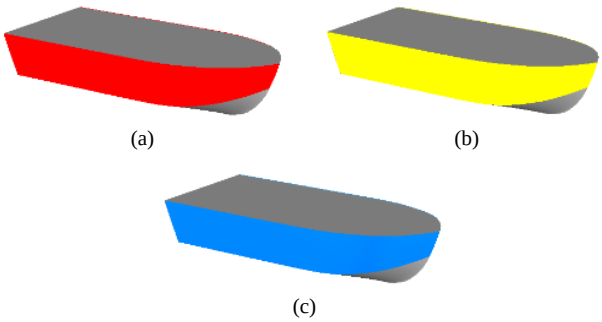

(a) (b)

(c)

Fig. 23. Shallow V hull design with dimensions: (a) Displacement and LOA; (b) Displacement and Beam; and (c) Displacement and Depth.

The design modeling results are presented in the design combination of hull type and main size regression results. For displacement and LOA, regression variations are grouped in design variation (a) for all hull types. So, sub-figure (a) in Figs. 20–23 is a hull design that uses variations in the size of displacement and LOA regression results. The same treatment applies to the displacement and beam regression variation in sub-figure (b) and displacement and depth in sub-figure (c).

E. Simulation Analysis

The following process is simulated after completing the design modeling process to see the hydrodynamic characteristics. The design resulted in 12 models of four hull types and three size variations. The simulation uses Maxsurf software. Resistance analysis on the hull uses the Savitsky method with a speed range of 0–50 knots during simulation. The simulation results are graphs of the relationship between speed, resistance, and ship power requirements. This resistance test aims to determine the design model with the slightest resistance and the most minimal power requirements.

Furthermore, ship stability testing uses Maxsurf Stability with a tilt angle range between 0–180°. In the large angle stability analysis, the load case setting used is the free trim load case. The conditions follow the Labuan Bajo water data, which has an average wave height of 1.4 m. The simulation data results are static stability values in the form of righting lever GZ curves. This simulation aims to determine the design model that has the best stability based on model variations.

Seakeeping testing is done by analyzing the ship's motion using Maxsurf Motion. The variation of wave direction used bow quartering seas (135°), ship speed of 10 knots, and wave height of 1.4 m. The type of wave spectrum chosen is JONSWAP spectra. The seakeeping simulation results are presented with RAO graphs in heave, roll, pitch motion, and motion sickness incidence graphs. This simulation aims to determine the ship's motion response to the specified water conditions.

After completing the simulation, the next step is a statistical calculation to analyze the influence of the hull shape and ship size on the simulation results. Multi-Attribute Decision Making (MADM) with the Simple Additive Weighting (SAW) method and sensitivity analysis are the alternatives. Both calculation methods aim to validate the effect of changes in hull shape and primary size on the performance of the ship's hydrodynamic characteristics.

V. Results

After the design modeling process is complete, the next step is to simulate the three factors that affect the hydrodynamic characteristics of the ship (resistance, stability, and seakeeping). At this stage, the simulation test results of all model variations will be compared. Each simulation's parameters and boundary conditions have the same status so that the simulation results represent each model variation.

A. Resistance Simulation

This test determines the amount of hull resistance when traveling on water. Simulation of resistance using the Savitsky method with a speed range in this simulation ranging from 0–50 knots. The resistance testing results on the reference ship are presented in Tables XIV–XV, while the speed comparison graph with resistance and power is in Fig. 24.

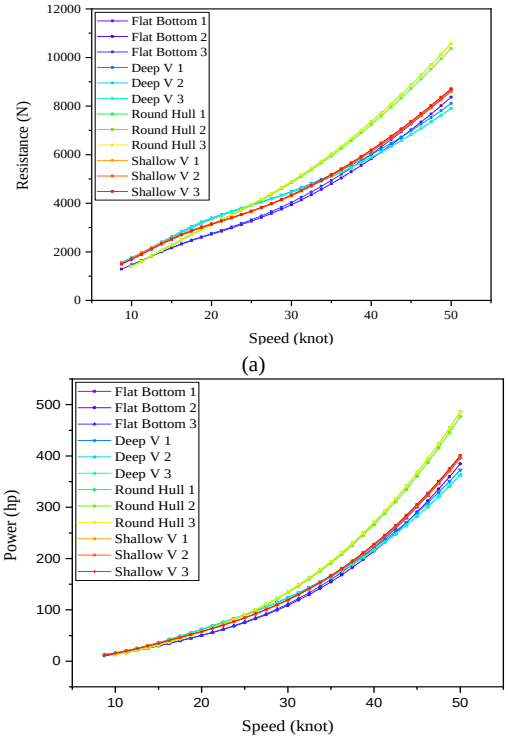

Fig. 24. Resistance graph of 12 hull variations: (a) Speed vs Resistance; and (b) Speed vs Power.

TABLE XIV. Speed vs Resistance

Model	Resistance (N)				
	V=10	V=20	V=30	V=40	V=50
Flat Bott. 1	1494.2	2735.3	3972.6	5909.5	8503.7
Flat Bott. 2	1461.4	2720.8	3940.5	5829.7	8365.2
Flat Bott. 3	1461.4	2748.6	4036.6	6017.1	8661.5
Deep V 1	1708.0	3348.4	4483.3	6000.9	8106.5
Deep V 2	1762.4	3392.8	4449.6	5885.0	7901.2
Deep V 3	1722.8	3358.7	4453.2	5894.1	7908.1
Round hull 1	1413.0	3126.9	4890.8	7352.5	10572.0
Round hull 2	1391.2	3104.5	4841.3	7236.9	10373.2
Round hull 3	1401.2	3121.4	4892.0	7354.2	10573.1
Shallow V 1	1738.8	3140.2	4307.2	6156.7	8672.4
Shallow V 2	1715.6	3158.7	4319.9	6128.1	8593.7
Shallow V 3	1689.7	3134	4333.3	6188.5	8707.0

TABLE XV. Speed vs Power

Model	Power (hp)				
	V=10	V=20	V=30	V=40	V=50
Flat Bott. 1	13.74	50.32	109.62	217.43	391.10
Flat Bott. 2	13.44	50.05	108.74	214.49	384.73
Flat Bott. 3	13.44	50.56	111.39	221.39	398.36
Deep V 1	15.71	61.60	123.71	220.79	372.83
Deep V 2	16.21	62.41	122.79	216.53	363.39
Deep V 3	15.84	61.78	122.88	216.86	363.71
Round hull 1	12.99	57.52	134.96	270.52	486.23
Round hull 2	12.79	57.11	133.59	266.27	477.08
Round hull 3	12.88	57.42	134.99	270.59	486.27
Shallow V 1	15.99	57.77	118.85	226.53	398.86
Shallow V 2	15.78	58.11	119.21	225.47	395.24
Shallow V 3	15.54	57.65	119.57	227.70	400.45

Based on the table above, it can be seen that the variation model that had the most significant resistance value and power requirement was round hull 3, with a value of 10573.1 N and 486.279 hp, respectively. The variation model with the lowest resistance value and power requirement was Deep V 3, which was 7901.24 N and 363.395 hp. At low-speed conditions, the Deep V Hull type has a high resistance value that tends to be higher than the round hull type but changes drastically when the speed is high. This issue is related to the characteristics of the Deep V Hull, which is included in the planning hull category. At higher speeds, the planning hull type has the characteristic of providing lift to the hull so that the area attached to the water surface will decrease, and automatically, the resistance value will decrease.

The data results showed that the higher the speed, the higher the total resistance value and the power required. The amount of resistance is proportional to the amount of power required. Based on the average amount of resistance and power for each hull model, hull types with average resistance and power requirements from the lowest value are flat bottom, deep v, shallow v, and round hull. For the sequence of dimensional size variations with the lowest resistance values and power requirements, namely displacement and beam, displacement and depth, and displacement and LOA.

B. Stability Simulation

Stability testing will simulate the hull's performance when under the influence of forces that usually occur due to wind or waves. The righting lever GZ curve results from the representation of the ship stability simulation shown in Fig. 25. The curve shows the relationship between the ship's tilt position and the GZ value. Then, the simulation result data is presented in Table XVI below.

TABLE XVI. STABILITY SIMULATION RESULTS

Model	Righting Lever Curve			
	GZ Max. (m)	α (•)	Area (m. •)	Angle of Vanishing Degree (•)
Flat Bott. 1	0.34	24.5	22.08	98.8
Flat Bott. 2	0.29	24.5	18.89	100.9
Flat Bott. 3	0.33	24.5	21.36	100.0
Deep V 1	0.44	55.5	23.29	97.0
Deep V 2	0.39	58.2	20.24	98.0
Deep V 3	0.43	57.3	22.19	97.7
Round hull 1	0.393	33.6	25.17	95.4
Round hull 2	0.34	33.6	20.01	96.4
Round hull 3	0.383	33.6	24.56	96.1
Shallow V 1	0.28	60	18.5	98.5
Shallow V 2	0.237	63.6	15.61	100.3
Shallow V 3	0.266	60.9	17.85	99.7

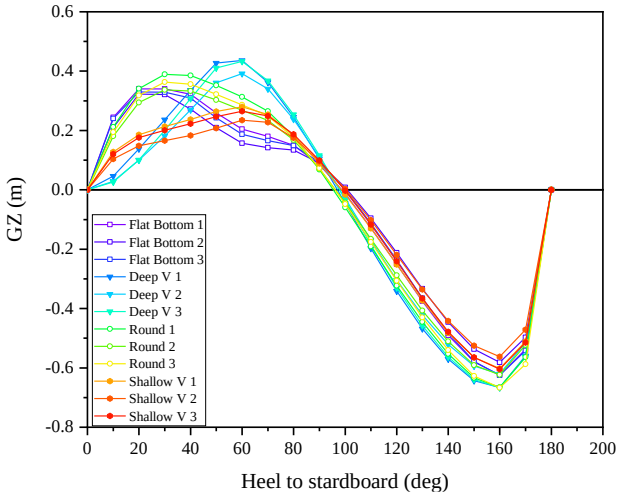

Fig. 25. Comparison graph of GZ values of 12 hull variations.

Based on the graph above, the results of stability simulations on 12 variation models produced varying data. There were four different curve trends in each simulated hull type. The character of the flat bottom and round hull curve lines looked similar, but there are differences in slope areas from 50° to 80°. Meanwhile, curve lines significantly differred in the shallow v and deep v models. The model variation with the maximum GZ value was Deep V 1 of 0.444 m with a tilt angle value of 55.5°. In comparison, the model variation with the lowest maximum GZ was the Shallow V 2 hull model with a value of 0.237 m at a ship tilt of 63.6°.

Based on the stability simulation results, the factor that affects the level of hull stability is the maximum GZ value. Positive GZ indicates that the ship has positive stability. The size of the GZ number can be a parameter of the hull stability level. The greater the GZ value, the better the ship's restoration ability when tilted and not easily overturned when receiving external forces. This statement is related to the three stability points, namely Gravity (G), Buoyancy (B), and Metacenter (M), which are indicators of the hull stability position. In addition, the angle of vanishing degree is also essential to determine the maximum tilt angle of the ship as a limit to the risk of irreversible ship tilt.

From the simulation data above, it can be concluded that the Deep V Hull model had the best stability test results. At the same time, the shallow v model gave a contrasting result with a comparison of the average value of max GZ, which was 0.424 m and 0.261 m. The other two hull types, namely flat bottom and round hull, had an excellent max GZ, but the tilt angle value when maximum stability was achieved was low. The size variation variables with the highest average max GZ were displacement and LOA, displacement and depth, displacement and beam. The beam value of each variation influenced this. The wider the beam value of the ship, the better the stability ability.

C. Seakeeping Simulation

The seakeeping simulation test aims to determine the ship's response to the specified water conditions. Seakeeping analysis will produce a Response Amplitude Operator (RAO) graph that describes the amplitude of the ship's response to various wave frequencies. In addition, the seakeeping test results can also predict the seasickness index due to the waves that hit the ship. Seakeeping analysis can provide insight into how the ship will respond. The simulation data results presented are Response Amplitude Operator (RAO) graphs on heave, roll, and pitch motion against wave frequency. In addition, seakeeping simulation testing also produces Motion Sickness Incidence (MSI).

The seakeeping simulation results on the heave motion were from a speed variation of 10 knots, the direction of the incident wave 135°, and a wave height of 1.4 m. The graph of heave motion RAO data results from 12 model variations is presented in Fig. 26.

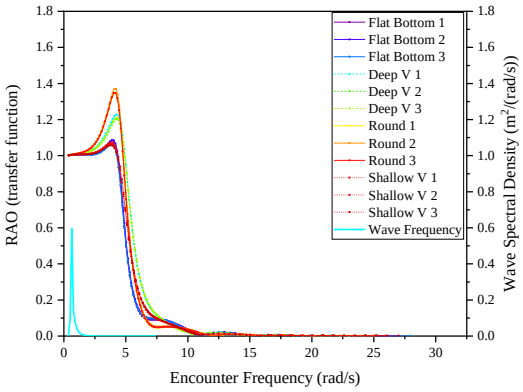

Fig. 26. RAO heaving motion graph of 12 hull variations.

Based on the graph above, the model variation that showed the lowest response amplitude was Shallow V 3. This model had a maximum RAO value of 1.05 with a wave frequency of 3.78 rad/s. At the same time, the ship model with the highest response amplitude was Round 2. The maximum RAO value of this model was 1.36, with a wave frequency of 4.07 rad/s. With the condition that the tested speed was relatively low in the direction of the incident wave 135°, the round hull model had the highest heaving motion response, followed by the deep v, flat bottom, and shallow v models.

This round hull design had a more convex bow shape and a relatively round or curved hull bottom shape. Then, the shallow v model had a V-shaped hull bottom shape with a smaller tilt angle. When analyzing the heaving motion (up and down of the ship on the z-axis) in wave conditions as above, it makes sense when the round hull model had a higher response. The round hull model had a more convex bottom surface shape than the shallow v model, so water waves will more easily lifted the round hull model than the shallow v with a V-shaped bottom that tended to split the water.

The seakeeping simulation results on roll motion were from a speed variation of 10 knots, incident wave direction of 135°, and wave height of 1.4 m. The graph of the results of roll motion RAO data from 12 variation models is presented in Fig. 27.

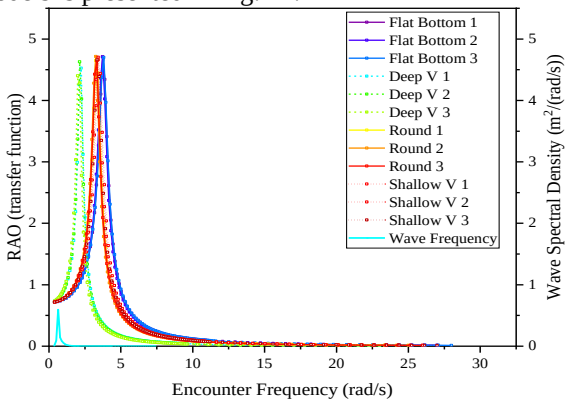

Fig. 27. RAO rolling motion graph of 12 hull variations.

Based on the graph above, the model variation that showed the lowest response amplitude was Deep V 3. This model had a maximum RAO value of 4.4 with a wave frequency of 2 rad/s. At the same time, the ship model with the highest motion response was Flat Bottom 1. The maximum RAO value of this model was 4.7, with an encounter frequency of 3.73 rad/s. The curves generated by each hull type mostly had similar trend lines with almost the same peak value but occurred at different wave frequencies.

The Deep V Hull model experienced the peak of the rolling motion response at the most minor wave frequency among the other models. This condition indicates that the deep v model tends to have rolling effects when it gets waves from the side of the ship (beam seas). This effect can be caused by the shape factor of the Deep V Hull, which has a basic V shape. With such a shape, the hull will be more easily swayed when waves hit due to the base of the hull being more pointed than the top. Compared to the flat bottom hull model, which has a flat bottom shape, it will be more difficult to be affected by waves from the side. It is evident from the results of the RAO graph above that the amplitude response occurs at a more extended frequency.

The seakeeping simulation results on the pitch motion were from the speed variation of 10 knots, the direction of the incident wave 135°, and the wave height of 1.4 m. The graph of the pitch motion RAO data results from 12 variation models are presented in Fig. 28.

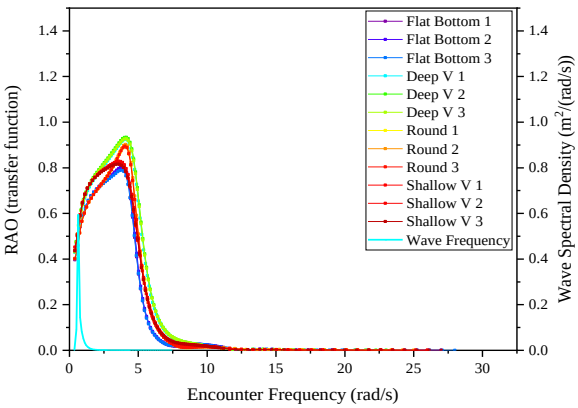

Fig. 28. RAO pitching motion graph of 12 hull variations.

Based on the graph above, the model variation that showed the lowest motion response was Flat Bottom 3. This model had a maximum RAO value of 0.78 with a wave frequency of 3.8 rad/s. At the same time, the ship model with the highest response amplitude was Deep V 2. The maximum RAO value of this model was 0.93, with a wave frequency of 4.13 rad/s. These results showed that when the wave direction occurred from the front tilted side (bow seas), the Deep V Hull had a higher response than other hull models, followed by shallow V, round hull, and flat bottom models. The V-hull types of Deep V and shallow V had similar characteristics.

Pitch motion (rotating around the y-axis) due to waves coming from the bow seas direction often occurs when the ship turns. The deep v and shallow V hull models have a basic "V" hull shape from bow to stern. When a wave passes the front of one side of the V hull, the pitch motion of the ship will push the back of the other side of the hull. This condition will occur synchronously within a specific wave frequency. However, it is different with a flat bottom and round hull shapes with a flat bottom shape. As a result of waves passing through the front of the hull, the pitch movement will be dampened by the shape of the surface of the flat back. As a result, the effect produced on the Deep V Hull shape is more significant than the flat bottom. Table XVII below summarizes the seakeeping motion response amplitude on 12 model variations.

TABLE XVII. RECAPITULATION OF SEAKEEPING DATA

Model	Criteria		
	Heave	Roll	Pitch
Flat Bott. 1	1.082	4.711	0.802
Flat Bott. 2	1.086	4.707	0.804
Flat Bott. 3	1.064	4.700	0.789
Deep V 1	1.227	4.524	0.925
Deep V 2	1.205	4.627	0.934
Deep V 3	1.209	4.400	0.927
Round hull 1	1.347	4.651	0.896
Round hull 2	1.369	4.715	0.902
Round hull 3	1.347	4.644	0.894
Shallow V 1	1.062	4.662	0.820
Shallow V 2	1.071	4.704	0.828
Shallow V 3	1.057	4.659	0.816

Leisure boats are vehicles used to move to tourist destinations or even travel on ships. In this case, passenger comfort in the ship design process needs to be considered. Through seakeeping simulation, we can review the level of passenger comfort with the Motion Sickness Incidence (MSI) graph. The test was conducted at a ship speed of 10 knots with a wave angle of 135° and a wave height of 1.4 m. The motion sickness incidence graphs of the 12 model variations are presented in Fig. 29.

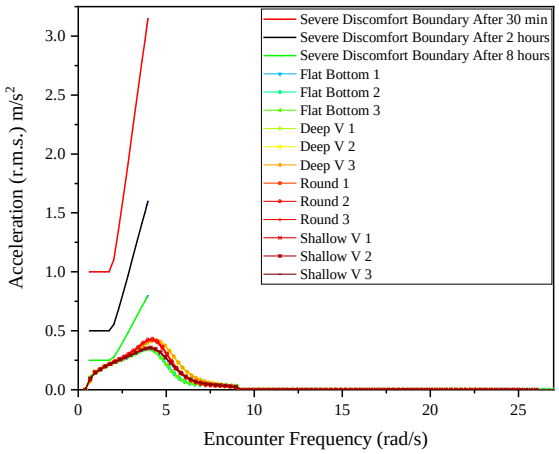

Fig. 29. Motion Sickness Incidence (MSI) graph of 12 hull variations.

Based on the MSI graph above, from all variations of the hull model, no curve line crossed the three discomfort limit lines. The Y-axis represents the severity of seasickness; the higher the level, the worse the potential for seasickness. A lower level indicates a better seasickness index. The hull type that had the highest response amplitude was the Round Hull 2 variation. This model had the highest acceleration value of 0.43 m/s^2 with an encounter frequency of 3.35 rad/s. The other model variations had the same curve trend. This research focused on the type of leisure ship that tourist uses. Usually, ships used for tourism more often use relatively low speeds. From the results of MSI simulations that have been carried out, all variation models have a low level of seasickness.

D. Multi Attribute Decision Making (MADM)

The MADM calculation aims to determine the best model variation (based on hull shape and size variation) from hydrodynamic testing. This method uses Simple Additive Weighting (SAW). Each type of simulation had a specific weight along with the needs of the ship. Giving weight to each MADM criterion is shown in Table XVIII.

TABLE XVIII. WEIGHTING VALUE ON EACH CRITERION

Criteria	Notation	Percentage
Resistance	C1	10%
Stability	C2	30%
Heaving	C3	15%
Rolling	C4	15%
Pitching	C5	15%
MSI	C6	15%

At the weight assignment stage, the resistance parameter got smaller than the stability and seakeeping parameters. The stability factor got a weight of 30% because the leisure boat carried tourist passengers, so the safety factor was a priority. The seakeeping factor was divided into four sub-criteria: heave, roll, pitch, and seakeeping. Each of these criteria got a weight of 15%. This factor had a very crucial role in terms of passenger comfort. Then, the resistance factor got a weight of 10% against the background of leisure boats that did not travel

long distances and relatively low ship speeds. However, this factor must be considered in the calculation.

TABLE XIX. PARAMETER VALUES FOR EACH VARIATION MODEL

Model	Criteria					
	C1	C2	C3	C4	C5	C6
Flat Bottom 1	2194.73	0.34	1.082	4.711	0.802	0.351
Flat Bottom 2	2162.07	0.29	1.086	4.707	0.804	0.353
Flat Bottom 3	2173.84	0.33	1.064	4.700	0.789	0.343
Deep V 1	2570.55	0.44	1.227	4.524	0.925	0.421
Deep V 2	2630.66	0.39	1.205	4.627	0.934	0.421
Deep V 3	2579.71	0.43	1.209	4.400	0.927	0.420
Round hull 1	2290.74	0.393	1.347	4.651	0.896	0.423
Round hull 2	2262.74	0.34	1.369	4.715	0.902	0.432
Round hull 3	2279.54	0.383	1.347	4.644	0.894	0.426
Shallow V 1	2561.81	0.28	1.062	4.662	0.820	0.353
Shallow V 2	2546.56	0.237	1.071	4.704	0.828	0.358
Shallow V 3	2516.12	0.266	1.057	4.659	0.816	0.350

Based on simulation results, these criteria were used as the basis for determining the best reference ship. The data from each test were used in the multi-attribute decision-making (MADM) calculation. The data used for resistance criteria were taken from the speed at 15 knots, and stability came from the GZ max value. Meanwhile, seakeeping data came from RAO amplitude values in heave, roll, pitch, and motion sickness incidence results. The model variation with the highest total value was the best model in the current study. Data from each simulation parameter is presented in Table XIX.

The next step is normalization to avoid data anomalies. For criteria C1 and C3 (resistance and seakeeping), the smallest data was chosen as a reference for normalization. For the C2 criteria, we decided on the most significant data because a good ship design has a low resistance value, seakeeping RAO peak point, and high stability. Normalization data for all model variations are presented in Table XX.

TABLE XX. DATA NORMALIZATION

Model	Criteria					
	C1	C2	C3	C4	C5	C6
Flat Bottom 1	0.985	0.773	0.977	0.934	0.984	0.976
Flat Bottom 2	1.000	0.659	0.974	0.935	0.981	0.971
Flat Bottom 3	0.995	0.750	0.993	0.936	1.000	1.000
Deep V 1	0.841	1.000	0.861	0.973	0.853	0.814
Deep V 2	0.822	0.886	0.877	0.951	0.845	0.815
Deep V 3	0.838	0.977	0.874	1.000	0.851	0.816
Round hull 1	0.944	0.893	0.785	0.946	0.880	0.810
Round hull 2	0.956	0.773	0.772	0.933	0.874	0.794
Round hull 3	0.948	0.870	0.785	0.947	0.883	0.804
Shallow V 1	0.844	0.636	0.995	0.944	0.962	0.970
Shallow V 2	0.849	0.539	0.987	0.935	0.953	0.956
Shallow V 3	0.859	0.605	1.000	0.944	0.967	0.980

Based on the normalized data, the total value of each reference ship model is summed up. From the summation results, the best design variation model can be determined based on MADM calculations. The results of the total value of all design variation models are presented in Table XXI.

TABLE XXI. MADM TOTAL VALUE

Model	Criteria					
	C1	C2	C3	C4	C5	C6
Flat Bottom 1	0.099	0.232	0.1465	0.1401	0.1476	0.1464
Flat Bottom 2	0.100	0.198	0.1460	0.1402	0.1472	0.1456
Flat Bottom 3	0.099	0.225	0.1489	0.1404	0.1500	0.1500
Deep V 1	0.084	0.300	0.1292	0.1459	0.1279	0.1221
Deep V 2	0.082	0.266	0.1316	0.1426	0.1268	0.1222
Deep V 3	0.084	0.293	0.1311	0.1500	0.1277	0.1224
Round hull 1	0.094	0.268	0.1177	0.1419	0.1320	0.1215
Round hull 2	0.096	0.232	0.1158	0.1400	0.1312	0.1191
Round hull 3	0.095	0.261	0.1177	0.1421	0.1324	0.1206
Shallow V 1	0.084	0.191	0.1492	0.1416	0.1443	0.1455
Shallow V 2	0.085	0.162	0.1480	0.1403	0.1429	0.1435
Shallow V 3	0.086	0.181	0.1500	0.1417	0.1451	0.1469

After obtaining the total value of the 12 hull variation models, the next step is ranking to determine the best model with the highest final score. The results of the ranking order of the 12 hull variation models can be seen in Table XXII.

Based on the calculation results of the MADM method, the model variation in the best position was Deep V 1 with a total value of 0.787. The model variation with the lowest ranking results was Shallow V 2, with a final value of 0.678. The test results of each hydrodynamic criterion and weighting values are very influential in MADM calculations. Of the four types of hull forms used, deep v was in the top position, followed by flat bottom, round hull, and shallow v. In each hull shape, variable size 1 (the result of the regression approach with displacement and LOA locking) consistently ranks first, followed by variations 3 (displacement and depth) and 2 (displacement and beam).

TABLE XXII. RESULTS OF THE BEST MODEL ORDER BASED ON MADM

Ranking	Model	Total Value
1	Deep V 1	0.787
2	Deep V 3	0.786
3	Flat Bottom 1	0.765
4	Flat Bottom 3	0.764
5	Round Hull 1	0.754
6	Deep V 2	0.749
7	Round Hull 3	0.748
8	Flat Bottom 2	0.731
9	Round Hull 2	0.714
10	Shallow V 1	0.710
11	Shallow V 3	0.704
12	Shallow V 2	0.678

E. Sensitivity Analysis

The influence of hull form and ship size variables on the results of each hydrodynamic characteristic can be known based on sensitivity analysis. The data from the calculation of this method is presented based on the types of resistance, stability, and seakeeping analysis. In the hull form variable, the data used as input value is the block coefficient (Cb). For the size variable, the input data represents the displacement volume. Table XXIII below is the result of the sensitivity analysis on resistance simulation.

TABLE XXIII. SENSITIVITY ANALYSIS RESULTS OF RESISTANCE PARAMETERS

Parameter	Variable	
	Hull form	Dimension
Coefficient	−3.1946	−28.5836
Standard error	0.1216	0.1770
P value	0.0030	0.2057
Significant F	0.0030	0.2057
R square	0.6008	0.1547

Based on the sensitivity analysis calculation table above, the influence of the hull form variable on resistance testing was more dominant than the size variable. This statement can be seen from the R Square value on the hull form variable, which was more significant than the size variable at 0.6008. The data was supported by the *p*-value and significant F results, below the critical value of 0.05. It showed sufficient evidence to confirm the effect/difference in the observed resistance test results. Unlike the size variable, the *p*-value and significant F of this variable were above the critical point of 0.05, which was 0.2057. Both variables had a small standard error value, namely 0.1216 and 0.1770, which means that the precision of the analysis coefficient in measuring the relationship between statistical variables was getting higher.

The results of these calculations can be used to support decisions based on a logical approach. A good hull shape can reduce hydrodynamic drag resistance when traveling in the water. Ships with smooth, tapered, and aerodynamic hull shapes usually have lower resistance. This statement can be seen from the resistance test results in Fig. 24 and Table XIV, where the Deep V Hull shape had a lower resistance value than the round hull shape. Indirectly, it also reduced the power requirement used to fight fluid resistance. Although the size of the vessel can affect the resistance, size is also associated with greater propulsion power that may be required to move a larger vessel. Thus, an increase in propulsion power can overcome the size effect. Furthermore, Table XXIV below present the results of the sensitivity analysis data based on the stability simulation.

Based on the table above, in testing the stability of the influence of the hull form variable, it was more dominant than the size variable. The R square value on the hull form variable was greater than the size variable, which is 0.5930. The higher the R Square value, the better the variable data that explains the test results. The p−value and significant F on the hull form variable were below the critical point of 0.05. It showed sufficient evidence to state that the effect/difference of the observed stability test results was accurate. At the same time as the hull form variable, the *p*-value and significant F of the size variable were above the 0.05 critical point of 0.2280. However, both variables had a relatively large standard error value of 10.8660 and 15.7824. This condition caused the coefficient precision value to be too large, namely −280.7444 and −2417.7935.

TABLE XXIV. SENSITIVITY ANALYSIS RESULTS OF STABILITY PARAMETERS

Parameter	Variable	
	Hull form	Dimension
Coefficient	−280.7444	−2417.7935
Standard error	10.8660	15.7824
P value	0.0033	0.2280
Significant F	0.0033	0.2280
R square	0.5930	0.1415

Ship stability is complex and involves many factors, including hull form and size. Hull form plays a vital role in ship stability. Ships that have a lower center of gravity tend to be more stable. Ship stability can be measured by knowing the relationship between the center of gravity and the buoyancy point. GZ data can represent this relationship, where a high GZ value indicates that the ship can recover from tilt and not quickly capsize. This statement follows the stability test results shown in Fig. 25 and Table XVI, which showed that the hull form variable significantly affected ship stability. The hull model with a deep v shape had the highest GZ value among other hull types. Then, Table XXV below will show the sensitivity analysis results based on heave motion parameters in seakeeping simulations.

TABLE XXV. SENSITIVITY ANALYSIS RESULTS OF SEAKEEPING HEAVE MOTION

Parameter	Variable	
	Hull form	Dimension
Coefficient	−1.2467	−8.4215
Standard error	0.1155	0.1274
p−value	0.1420	0.5919
Significant F	0.1420	0.5919
R square	0.2026	0.0297

These results showed that the coefficients' precision level in describing the sensitivity analysis calculation model was relatively high. This result was indicated by the standard error values of the two models, which were small, namely 0.1155 and 0.1274. The resulting p−value and significant F values exceeded the predetermined critical point of 0.05, so the null hypothesis assumption was correct (the null hypothesis is the assumption that there is no significant effect of change in the data). The sensitivity analysis results of seakeeping testing for heave motion on the hull form variable had a more significant

influence than the size variable. However, the resulting R Square value difference was close, 0.2026, compared to 0.0297.

Heave motion is the vertical movement of the ship caused by sea waves. The variables given in this study are hull form and ship size variations. Based on the given size variables, the differences in the given variations were not far adrift of each other, especially LOA. The longship size can handle heave motion better because it has more buoyancy under the water's surface. As a result of the LOA variation was not too far adrift, the effect on the calculation analysis became insignificant. In contrast, the hull form variable which had four different hull types. Each type of hull has its characteristics in handling heave motion, as shown in the analysis of heave motion in Fig. 21. Furthermore, Table XXVI below shows the results of sensitivity analysis on roll motion in seakeeping simulations.

TABLE XXVI. SENSITIVITY ANALYSIS RESULTS OF SEAKEEPING ROLL MOTION

Parameter	Variable	
	Hull form	**Dimension**
Coefficient	−2.020	−191.641
Standard error	2.228	153.599
p-value	0.386	0.240
Significant F	0.386	0.240
R square	0.075	0.134

Based on the sensitivity analysis calculation table above, the influence of the size variable on seakeeping testing for roll motion was more dominant than the hull form variable. This statement can be seen from the R Square value on the size variable, which was greater than the hull form variable, 0.4081. The data was supported by the results of the *p*-value and significant F, which was below the critical value of 0.05, which is 0.0253. It showed sufficient evidence that the effect/difference in seakeeping test results, especially in the roll motion observed, was real. Unlike the size variable, the *p*-value and F significance of this variable were above the critical point of 0.05, which was 0.1422. Both variables had small standard error values of 0.0870 and 0.0749, which means that the precision of the analysis coefficient in measuring the relationship between statistical variables is better.

Roll motion is sideways (around the x-axis) due to waves from the ship's side. The stability factor is interrelated with roll motion. In this case, a hull model that had wider characteristics can make the ship more stable in handling roll motion. As shown in Table XVI and Fig. 25, model variations 1 and 3 in each hull type had higher GZ values and lower amplitudes, which means better stability. This condition was because model variations 1 and 3 had higher beam values. Based on this analysis, the calculations produced in the sensitivity analysis made sense. Next, the sensitivity analysis results of pitch motion in the seakeeping simulation are shown in Table XXVII.

Based on the Table XXVII, in seakeeping tests, especially in pitch motion, the influence of the hull form variable was more dominant than the size variable. The R^2 value on the hull form variable was greater than the size variable, which was 0.4824. The higher the R^2 value, the better the variable data that explained the test results. The *p*-value and significant F on the hull form variable were below the critical point of 0.0121. It showed sufficient evidence to state that the effect/difference of the observed seakeeping test results was accurate. In contrast to the hull form variable, the *p*-value and significant F of the size variable were above the 0.05 critical point of 0.2736. Both variables had relatively low standard error values of 0.0422 and 0.0551. So that the coefficient value used to measure the relationship between variables was more precise.

TABLE XXVII. SENSITIVITY ANALYSIS RESULTS OF SETABLE 1 AKEEPING PITCH MOTION

Parameter	Variable	
	Hull form	**Dimension**
Coefficient	−0.8726	−7.6174
Standard error	0.0422	0.0551
p-value	0.0121	0.2736
Significant F	0.0121	0.2736
R square	0.4824	0.1182

Pitch motion is the swinging motion of the ship along its longitudinal axis (y-axis). If analyzed logically, the areas that are very influential in pitch motion are the bow and stern of the hull. A blunt hull at the front and sharp at the back can affect the pitch motion. Bow shapes that tend to be flat/blunt can reduce pitch motion better. Fig. 28 shows that the flat bottom hull shape had a lower amplitude than the Deep V model. The results of this observation were supported by the sensitivity analysis calculation above, which stated that the hull form variable had more influence on seakeeping testing for pitch motion.

VI. CONCLUSIONS

In this study, two variables, namely hull form and size, were analyzed to determine their effects on the hydrodynamic characteristics of the hull for the intended use of leisure boats. The hydrodynamic criteria for determining the hull characteristics included resistance, stability, and seakeeping. The hull form variations were flat bottom, deep v, round hull, and shallow v. In size variation, this research used three types of variations from the regression approach with LOA, beam, and depth locking parameters. Based on the results of the research that had been done, it can be concluded that:

- The resistance simulation results showed that the variation model with the lowest resistance value and power requirement at maximum speed was Deep V 3, which was 7901.24 N and 363.395 hp. The higher the ship's speed, the greater the resistance value and power requirements. The Deep V Hull was included in the planning hull category, where one of its

advantages was the ability to minimize resistance during high-speed conditions.

- Stability testing will show the ability of hull stability in the encounter of waves. Ships with good stability can restore from tilt and not quickly capsize. The model variation with the highest max GZ value was Deep V 1 of 0.444 m with a tilt angle value 55.5°. The size of the max GZ value can affect the hull's stability—the wider the hull beam size, the better the stability ability.
- In the seakeeping test, the Shallow V 3 model variation gave the lowest heave motion amplitude response of 1.0573. The model variation with the slightest amplitude response for roll motion was Deep V 3 of 4.4008. Furthermore, in pitch motion, the Flat Bottom 3 model variation had the lowest amplitude response with a value of 0.7894. For motion sickness incidence (MSI) results, the hull model with the lowest seasickness index was Flat Bottom 3, with a value of 0.3431. There was no dominant hull model for all types of seakeeping motions. Each hull shape had its advantages in dealing with water conditions.
- The calculation results of the Multi-Attribute Decision Making (MADM) method showed that the model variation with the highest score was Deep V 1 with a total value of 0.787. The weighting emphasizes aspects of stability and seakeeping following the intended use of leisure vessels that prioritize safety and comfort. The Deep V 1 model variation excelled in the stability aspect with the highest weight value and can handle roll motion in seakeeping testing with the second-best weight value. The combination of good test results and proper weighting resulted in the Deep V 1 model variation being the best in the MADM method ranking.
- Calculation of sensitivity analysis on resistance testing showed the results of hull form variables were more influential on the resistance results with an R square value of 0.6008. The slim, tipped, and aerodynamic hull shape can reduce the resistance given by the fluid. Then, the stability test showed that the hull form variable affected the ship's stability ability more than the size variable. The R square comparison value of both was 0.5930 and 0.1415. Ships with a hull form with a lower center of gravity had better stability. In the calculation of sensitivity analysis for each seakeeping motion, the hull form variable had more effect on heave and pitch movements with R square values of 0.2026 and 0.4824, respectively. In comparison, the size variable significantly impacted the type of roll motion with a ratio of R square values of 0.4081 and 0.2024. Roll motion is closely related to stability. Ships that have a wider beam have better stability capabilities. Meanwhile, the heave and pitch movements are more determined by the hull's form, especially at the bow and stern.

Conflict of Interest

The authors declare no conflict of interest.

Author Contributions

M.A.L.: Conceptualization; Investigation; Formal analysis; Validation; Methodology; Data curation; Writing—original draft; A.R.P.: Supervision; Writing—original draft; Writing—review & editing; Software; Funding acquisition; Project administration; E.M.M.: Supervision; Conceptualization; Investigation; T.M.: Conceptualization; Investigation; Project administration; N.M.: Supervision; Conceptualization; Methodology; Writing—original draft; Funding acquisition; Project administration; H.D.: Conceptualization; Investigation; Visualization; Writing—original draft; Q.T.D.: Conceptualization; Investigation; Project administration; S.J.B.: Conceptualization; Investigation; A.B.: Conceptualization; Investigation; Visualization. All authors had approved the final version.

Nomenclatures

C_f	Coefficient of frictional resistance
C_v	Coefficient of viscous resistance
F_n	Froude number
G	Center of gravity
g	Gravity acceleration (m/s^2)
GZ	Distance of point G to Z (m)
K	Turbulence kinetic energy (m^2/s^2)
L	Length of waterline (m)
m_4	Spectral moment of the ship
R_f	Frictional resistance (N)
R_n	Reynold number
R_v	Viscous resistance (N)
R_w	Wave resistance (N)
S	Wetted area (m^2)
V	Displacement volume (m^3)
v	Speed (m/s)
	Greek symbols
Δ	Displacement (kg)
β	Deadrise angle (•)
ζ_a	Amplitude of the incident wave (•)
$\emptyset_a$	Ship motion response amplitude
λ	Leeway angle (•)
μ	Water viscosity (m^2/s)
ρ	Water density(kg/m^3)
τ	Trim angle (•)
φ	Heel angle (•)

References

[1] A. Kodir, A. Tanjung, I. K. Astina, M. A. Nurwan, A. G. Nusantara, and R. Ahmad. "The dynamics of access on tourism development in labuan bajo, indonesia," *Geo Journal of Tourism and Geosites*, vol. 29, no. 2, pp. 662–677, 2020.

[2] N. M. U. Dwipayanti, A. Nastiti, H. Johnson, J. Loehr, M. Kowara, P. D. Rozari, S. Vada, W. Hadwen, M. A. T. Nugraha, and B. Powell, "Inclusive WASH and sustainable tourism in Labuan Bajo, Indonesia: Needs and opportunities," *Journal of Water, Sanitation and Hygiene for Development*, vol. 12, no. 5, 2022.

[3] A. E. Nyoko and R. P. Fanggidae, "The potentıal and opportunıtıes of tourısm entrepreneurshıp in labuan bajo," *Psychology and Education*, vol. 58, no. 5, pp. 1553–6939, 2021.
[4] P. Aisyah, I. Rizkiansyah, Y. Yuliantini, and L. Mafrudoh, "A sea transportation analysis to support tourism in labuan bajo," *Advances in Transportation and Logistics Research*, vol. 5, pp. 226–236, 2022.
[5] B. A. B. Hisham, S. Ahmad, and A. R. A. Ghani. "Stability and power resistance of a multi-hull tourism boat," *Journal of Applied Engineering Design and Simulation*, vol. 2, no. 1, pp. 43–50, 2022.
[6] G. K. Riungu, J. C. Hallo, K. F. Backman, M. Brownlee, J. A. Beeco, and L. R. Larson, "Water-based recreation management: A normative approach to reviewing boating thresholds," *Lake and Reservoir Management*, vol. 36, no. 2, pp. 139–154, 2020.
[7] T. Olgaç and O. Bayazit, "An investigation of the maritime accident in the aegean sea turkish search and rescue region," *Aquatic Research*, vol. 6, no. 2, pp. 83–96, 2023.
[8] A. S. Moerwanto and T. Junoasmono, "Integrated tourism infrastructure development strategy," *Jurnal HPJI*, vol. 3, no. 2, pp. 67–78, 2017.
[9] World Economic Forum. The Travel and Tourism Competitiveness Report 2019: Travel and Tourism at a Tipping Point. [Online]. Available: https://www.weforum.org/reports/the-travel-tourism-competitiveness-report-2019
[10] S. Jeong and H. Kim, "Development of an efficient hull form design exploration framework," *Mathematical Problems in Engineering*, 838354, 2013.
[11] J. H. Ang, C. Goh, and Y. Li, "Hull form design optimization for improved efficiency and hydrodynamic performance of 'ship-shaped' offshore vessels," in *Proc. International Conference on Computer Applications in Shipbuilding*, 2015, pp. 71–80.
[12] R. I. Julianto, T. Muttaqie, R. Adiputra, S. Hadi, R. L. L. G. Hidajat, and A. R. Prabowo, "Hydrodynamic and structural investigations of catamaran design," *Procedia Structural Integrity*, pp. 93–100, 2020.
[13] A. Mandru and F. Pacuraru, "The effect of appendages on ship resistance," in *Proc. IOP Conference Series: Materials Science and* Engineering, vol. 1182**,** no. 1, 2021.
[14] R. A. Febrianto, A. R. Prabowo, S. J. Baek, and R. Adiputra, "Analysis of monohull design characteristics as supporting vessel for the COVID-19 medical treatment and logistic," *Transportation Research Procedia*, vol. 55, pp. 699–706, 2021.
[15] T. Rahmaji, A. R. Prabowo, N. Muhayat, T. Tuswan, and T. Putranto, "Effect of bilge keel variations on the designed fast patrol boats to hull resistance and stability behaviours," in *Proc. IOP Conference Series: Earth and Environmental Science*, vol. 1166, 2023.
[16] D. Maulud and A. M. Abdulazeez, "A review on linear regression comprehensive in machine learning," *Journal of Applied Science and Technology Trends*, vol. 1, no. 4, pp. 140–147, 2020.
[17] Y. Kim, S. Steen, and H. Muri, "A novel method for estimating missing values in ship principal data," *Ocean Engineering*, vol. 251, no. 110979, 2022.
[18] A. Dogrul, S. Song, and Y. K. Demirel, "Scale effect on ship resistance components and form factor," *Ocean Engineering*, vol. 209, 107428, 2020.
[19] A. F. Molland, S. R. Turnock, and D. A. Hudson, *Ship Resistance and Propulsion*, Cambridge University Press, 2017.
[20] S. Beji, "Formulation of wave and current forces acting on a body and resistance of ships," *Ocean Engineering*, vol. 218, 108121, 2020.
[21] A. S. Pratama, A. R. Prabowo, N. Muhayat, T. Putranto, and T. Tuswan, "Analysis of hull performance on fast patrol boat with an extended study of survivability under damaged conditions," in *Proc. IOP Conference Series: Earth and Environmental Science*, 2023, vol. 1166.
[22] Z. Liu, W. Liu, Q. Chen, F. Luo, and S. Zhai, "Resistance reduction technology research of high speed ships based on a new type of bow appendage," *Ocean Engineering*, vol. 206, 107246, 2020.
[23] D. M. Prabowoputra, A. R. Prabowo, I. Yaningsih, D. D. D. P. Tjahjana, F. B. Laksono, R. Adiputra, and H. Suryanto, "Effect of blade angle and number on the performance of bánki hydro-turbines: Assessment using CFD and FDA approaches," *Evergreen*, vol. 10, no. 1, pp. 519–530, 2023.
[24] J. Carlton, *Marine Propellers and Propulsion*, Butterworth-Heinemann, 2018.
[25] Q. Zeng, R. Hekkenberg, C. Thill, and H. Hopman, "Scale effects on the wave-making resistance of ships sailing in shallow water," *Ocean Engineering*, vol. 212, 107654, 2020.
[26] A. R. Prabowo, E. Martono, T. Muttaqie, T. Tuswan, and D. M. Bae, "Effect of hull design variations on the resistance profile and wave pattern: a case study of the patrol boat vessel," *Journal of Engineering Science and Technology*, vol. 17, no. 1, pp. 106–126, 2022.
[27] F. Ahlstrand and E. Lindbergh, "Methods to predict hull resistance in the process of designing electric boats," *KTH Royal Institute of Technology*, 2020.
[28] R. I. Julianto, A. R. Prabowo, N. Muhayat, T. Putranto, and R. Adiputra, "Investigation of hull design to quantify resistance criteria using Holtrop's regression-based method and Savitsky's mathematical model: A study case of fishing vessels," *Journal of Engineering Science and Technology*, vol. 16, no. 1, pp. 1426–1443, 2021.
[29] A. Bahatmaka, D. J. Kim, A. R. Prabowo, and M. T. Zaw, "Investigation on the performance of the traditional Indonesian fishing vessel," in *Proc. MATEC Web of Conferences*, vol. 159, 02056, 2018.
[30] J. He, H. Wu, C. Ma, C. J. Yang, R. Zhu, W. Li, and F. Noblesse, "Froude number, hull shape, and convergence of integral representation of ship waves," *European Journal of Mechanics-B/Fluids*, vol. 78, pp. 216–229, 2019.
[31] M. Terziev, T. Tezdogan, and A. Incecik, "Scale effects and full-scale ship hydrodynamics: A review," *Ocean Engineering*, vol. 245, 110496, 2022.
[32] A. M. Halawa, B. Elhadidi, and S. Yoshida, "Aerodynamic performance enhancement using active flow control on DU96-W-180 wind turbine airfoil," *Evergreen*, vol. 5, no. 1, pp. 16–24, 2018.
[33] S. Kaushik, V. Uniyal, A. K. Verma, A. K. Jha, S. Joshi, M. Makhloga, and S. Pal, "Comparative experimental and CFD analysis of fluid flow attributes in mini channel with hybrid CuO+ ZnO+ H_2O nano fluid and (H_2O) base fluid," *Evergreen*, vol. 10, no. 1, pp. 182–195, 2023.
[34] X. Zhang, L. Sun, C. Sun, C. Wang, and C. Chen, "Study on the influence of the moonpool on the smooth water resistance performance of the ship," *Ocean Engineering*, vol. 237, 109590, 2021.
[35] K. Johansen and B. M. Batalden, "Active learning for enhanced understanding of Ship damage stability," in *Proc. 6th Teaching and Education Conference*, 2018.
[36] P. Ruponen. *Principles of Ship Buoyancy and Stability*, Aalto University, 2021.
[37] P. Ruponen, T. Manderbacka, and D. Lindroth, "On the calculation of the righting lever curve for a damaged ship," *Ocean Engineering*, vol. 149, pp. 313–324, 2018.
[38] H. Luhmann and J. Pöttgen, "Design for safety and stability," in *Proc. Twelfth International Conference on the Stability of Ships and Ocean Vehicles*, 2015.
[39] B. Santoso, R. Romadoni, S. Suzdayan, and P. Nasution, "Risk assessment fishing vessel based for the intact ship stability," in *Proc. IOP Conference Series: Earth and Environmental Science*, vol. 934, 2021.
[40] S. Huang, J. Jiao, and C. Chen, "CFD prediction of ship seakeeping behavior in bi-directional cross wave compared with in uni-directional regular wave," *Applied Ocean Research*, vol. 107, 2021.
[41] I. P. S. Asmara and M. Adam, "Seakeeping and resistance analysis of 1200 GT passenger ship fitted with NACA 4412 stern foil using CFD method," in *Proc. IOP Conference Series: Materials Science and Engineering*, vol. 1175, 2021.
[42] H. Nubli, F. S. Utomo, H. Diatmaja, A. R. Prabowo, U. Ubaidillah, D. D. Susilo, Wibowo, T. Muttaqie, and F. B. Laksono, "Design of the bengawan Unmanned Vehicle (UV) roboboat: Mandakini neo," *Mekanika: Majalah Ilmiah Mekanika*, vol. 21, pp. 64–74, 2022.
[43] N. Nurhasanah, B. Santoso, R. Romadhoni, and P. Nasutioni, "Seakeeping analysis of hull rounded design with multi-chine model on fishing vessel," in *Proc. IOP Conference Series: Earth and Environmental Science*, 2020, vol. 430.

[44] V. Piscopo and A. Scamardella, "The overall motion sickness incidence applied to catamarans," *International Journal of Naval* Architecture *and Ocean Engineering*, vol. 7, 2015.
[45] L. Ibinabo and D. T. Tamunodukobipi, "Determination of the response amplitude operator (s) of an FPSO," *Engineering*, vol. 11, 2019.
[46] H. Diatmaja, A. R. Prabowo, N. Muhayat, T. Tuswan, and T. Putranto. "Fast ship prototype design simulation with fin stabilizer on hydrodynamic characteristics for ship realization planning," IOP *Conference Series: Earth and Environmental Science*, vol. 1166, 01247, 2023.
[47] K. Bhawsinka. "Maneuvering simulation of displacement type ship and planning hull," *Memorial University of Newfoundland*, 2008.
[48] S. Brizzolara and D. Bruzzone, "Hydrodynamic optimisation of high-speed trimaran hull forms," in *Proc. the Eighteenth International Offshore and Polar Engineering Conference*, 2008, vol. 6, no. 11, 108296.
[49] Z. Xu, "On multi-period multi-attribute decision making," *Knowledge-Based Systems*, vol. 21, no. 2, pp. 164–171, 2008.
[50] E. K. Zavadskas, A. Kaklauskas, Z. Turskis, and J. Tamošaitienė, "Multi-attribute decision-making model by applying grey numbers," *Informatica*, vol. 20, pp. 305–320, 2009.
[51] A. Saltelli, "Sensitivity analysis: Could better methods be used?," *Journal of Geophysical Research*, vol. 104, pp. 3789–3793, 1999.
[52] M. I. Hanif, R. Adiputra, A. R. Prabowo, Y. Yamada, and N. Firdaus, "Assessment of the ultimate strength of stiffened panels of ships considering uncertainties in geometrical aspects: Finite element approach and simplified formula," *Ocean Engineering*, vol. 286, 115522, 2023.
[53] Q. T. Do, T. Ghanbari-Ghazijahani, and A. R. Prabowo, "Developing empirical formulations to predict residual strength and damages in tension-leg platform hulls after a collision," *Ocean Engineering*, vol. 286, 115668, 2023.
[54] Y. M. Lutfi, R. Adiputra, A. R. Prabowo, E. Erwandi, N. Muhayat, "Assessment of the stiffened panel performance in the OTEC seawater tank design: Parametric study and sensitivity analysis," *Theoretical and Applied Mechanics Letters*, vol. 13, 100452, 2023.
[55] Baja Marine. Outlaw Models. BajaMarine.com, Red Shark Digital. (2020). [Online]. Available: https://bajamarine.com/outlaw-models
[56] Chaparral Boat. [Online]. Available: https://www.chaparralboats.com/Chaparral-Boat.php?id=730andaction=tab_highlightsandcountry=500
[57] Rand Boat. [Online]. Available: https://www.randboats.com/boats/leisure-28
[58] Master Craft. [Online]. Available: https://www.mastercraft.com/boats/x26/
[59] Xoboats. [Online]. Available: https://xoboats.com/xo-fleet/dscvr-9/
[60] T. Rahmaji, A. R. Prabowo, T. Tuswan, T. Muttaqie, N. Muhayat, and S. J. Baek, "Design of fast patrol boat for improving resistance, stability, and seakeeping performance," *Designs*, vol. 6, 2022.
[61] A. S. Pratama, A. R. Prabowo, T. Tuswan, R. Adiputra, N. Muhayat, B. Cao, and I. Yaningsih. "Fast patrol boat hull design concepts on hydrodynamic performances and survivability evaluation," *Journal of Applied Engineering Science*, pp. 1–31, 2023.